Mon. Not. R. Astron. Soc. **000**, 1–15 (2003) Printed 7 April 2004 (MN LATEX style file v2.2)

Estimating galaxy cluster magnetic fields by the classical and hadronic minimum energy criterion

C. Pfrommer⋆ and T. A. Enßlin⋆
Max-Planck-Institut für Astrophysik, Karl-Schwarzschild-Straße 1, Postfach 1317, 85741 Garching, Germany

7 April 2004

arXiv:astro-ph/0404119 v1 6 Apr 2004

ABSTRACT
We wish to estimate magnetic field strengths of radio emitting galaxy clusters by minimising the non-thermal energy density contained in cosmic ray electrons (CRe), protons (CRp), and magnetic fields. The *classical* minimum energy estimate can be constructed independently of the origin of the radio synchrotron emitting CRe yielding thus an absolute minimum of the non-thermal energy density. Provided the observed synchrotron emission is generated by a CRe population originating from hadronic interactions of CRp with the ambient thermal gas of the intra-cluster medium, the parameter space of the *classical* scenario can be tightened by means of the *hadronic* minimum energy criterion. For both approaches, we derive the theoretically expected tolerance regions for the inferred minimum energy densities. Application to the radio halo of the Coma cluster and the radio mini-halo of the Perseus cluster yields equipartition between cosmic rays and magnetic fields within the expected tolerance regions. In the hadronic scenario, the inferred central magnetic field strength ranges from 2.4 μG (Coma) to 8.8 μG (Perseus), while the optimal CRp energy density is constrained to 2% ± 1% of the thermal energy density (Perseus). We discuss the possibility of a hadronic origin of the Coma radio halo while current observations favour such a scenario for the Perseus radio mini-halo. Combining future expected detections of radio synchrotron, hard X-ray inverse Compton, and hadronically induced γ-ray emission should allow an estimate of volume averaged cluster magnetic fields and provide information about their dynamical state.

Key words: magnetic fields, cosmic rays, radiation mechanisms: non-thermal, elementary particles, galaxies: cluster: individual: Coma (A 1656), Perseus (A 426)

1 INTRODUCTION

Clusters of galaxies harbour magnetised plasma. In particular, the detection of diffuse synchrotron radiation from radio halos or relics provides evidence for the existence of magnetic fields within the intra-cluster medium (ICM) (for a review, see Carilli & Taylor 2002). Since the detection rate of radio halos in galaxy clusters seems to be of the order of 30% for X-ray luminous clusters (Giovannini et al. 1999), the presence of magnetic fields appears to be common. Based on these observations, Enßlin & Röttgering (2002) developed a redshift dependent radio halo luminosity function and predicted large numbers of radio halos to be detected with future radio telescopes.

A different piece of evidence comes from Faraday rotation which arises owing to the birefringent property of magnetised plasma causing the plane of polarisation to rotate for a nonzero magnetic field component along the propagation direction of the photons (Clarke et al. 2001). However, the accessible finite windows given by the extent of the sources emitting polarised radiation are a limitation of this method. The derived magnetic field strengths depend on the unknown magnetic field autocorrelation length which has to be deprojected from the observed two dimensional Faraday rotation measure maps using certain assumptions (see, however, Enßlin & Vogt 2003; Vogt & Enßlin 2003). A different approach is given by the energy equipartition argument if a particular cluster exhibits diffuse radio synchrotron emission. The method assumes equal energy densities of cosmic ray electrons and magnetic fields in order to estimate volume averaged magnetic field strengths.

The minimum energy criterion is a complementary method. It is based on the idea of minimising the non-thermal energy density contained in cosmic ray electrons (CRe), protons (CRp), and magnetic fields by varying the magnetic field strength. As one boundary condition, the implied synchrotron emissivity is required to match the observed value. Additionally, a second boundary condition is required mathematically which couples CRp and CRe. For the classical case, a constant scaling factor between CRp and CRe energy densities is assumed. However, if the physical connection between CRp and CRe is known or assumed, a physically better motivated criterion can be formulated. As such a case, we introduce the mini-

⋆ e-mail: pfrommer@mpa-garching.mpg.de (CP); ensslin@mpa-garching.mpg.de (TAE)

© 2003 RAS

mum energy criterion within the scenario of hadronically generated CRe.

Classically, the equipartition/minimum energy formulae use a fixed interval in radio frequency in order to estimate the total energy density in cosmic ray electrons (CRe), a purely observationally motivated procedure (Burbidge 1956; Pacholczyk 1970). However, this approach has a drawback when comparing different field strengths between galaxy clusters because a given frequency interval corresponds to different CRe energy intervals depending on the magnetic field strengths (Beck 2001). For this reason, variants of the minimum energy criterion have been studied in order to place the magnetic field estimates on more physical grounds, based then on assumptions such as the fixed interval in CRe energy (Pohl 1993; Beck et al. 1996; Brunetti et al. 1997). The modified classical minimum energy criterion does not specify a particular energy reservoir of the CRe. However, this apparent model-independence is bought dearly at the cost of the inferred magnetic field strength depending on unknown parameters like the lower energy cutoff of the CRe population or the unknown contribution of CRp to the non-thermal energy density. In the following, we use the term *classical minimum energy criterion* in its modified version, including e.g. a fixed interval in CRe energy.

Natural candidates for acceleration mechanisms providing a highly-relativistic particle population are strong structure formation and merger shocks (e.g., Harris et al. 1980; Sarazin 1999) or reacceleration processes of 'mildly' relativistic CRe ($\gamma_e \simeq 100 - 300$) being injected over cosmological timescales into the ICM. Owing to their long lifetimes of a few times 10^9 years, these mildly relativistic CRe can accumulate within the ICM (see Sarazin 2002, and references therein), until they experience continuous in-situ acceleration via resonant pitch angle scattering by turbulent Alfvén waves as originally proposed by Jaffe (1977) and reconsidered by Schlickeiser et al. (1987), Brunetti et al. (2001), Ohno et al. (2002), and Kuo et al. (2003). However, this reacceleration scenario also faces challenges as recent results imply: Brunetti et al. (2003) show, that if the CRp-to-thermal energy density ratio were more than a few percent, Alfvén waves would be damped efficiently such that the reacceleration mechanism of the electrons is inefficient. Because nearly all conceivable electron acceleration mechanisms produce a population of CRp which accumulates within the clusters volume, this represents an efficient damping source of Alfvén waves.[1] Kuo et al. (2004) presented an interesting line of argumentation to investigate the nature of radio halos by comparing the observed and statistically predicted population. This approach might allow to measure the life time of radio halos and thus help to conclude their physical origin with a future flux-limited, controlled, and homogeneous radio halo sample.

In this work, we examine a minimum energy criterion within another specific model for the observed extended radio halos of $\sim$ Mpc size: Hadronic interactions of CRp with the ambient thermal gas produce secondary electrons, neutrinos, and γ-rays by inelastic collisions taking place throughout the cluster volume. These secondary CRe would generate radio halos through synchrotron emission (Dennison 1980; Vestrand 1982; Blasi & Colafrancesco 1999; Dolag & Enßlin 2000; Miniati et al. 2001; Pfrommer & Enßlin 2004). This scenario is motivated by the following argument: The radiative lifetime of a CRe population in the ICM, generated by direct shock acceleration, is of the order of 10^8 years for $\gamma_e \sim 10^4$. This is relatively short compared to the required diffusion timescale needed to account for such extended radio phenomena (Brunetti 2002). On the other hand, the CRp are characterised by lifetimes of the order of the Hubble time, which is long enough to diffuse away from the production site and to be distributed throughout the cluster volume to which they are confined by magnetic fields (Völk et al. 1996; Enßlin et al. 1997; Berezinsky et al. 1997). The magnetic field strength within this scenario is obtained by analogy with the classical minimum energy criterion while combining the CRp and CRe energy densities through their physically connecting process. Apart from relying on the particular model, the inferred magnetic field strengths do not depend strongly on unknown parameters in this model.[2]

The philosophy of these approaches is to provide a criterion for the energetically least expensive radio synchrotron emission model possible for a given physically motivated scenario. To our knowledge, there is no first principle enforcing this minimum state to be realised in Nature. However, our minimum energy estimates are interesting in two respects: First, these estimates allow scrutinising the hadronic model for extended radio synchrotron emission in clusters of galaxies. If it turns out that the required minimum non-thermal energy densities are too large compared to the thermal energy density, the hadronic scenario will become implausible to account for the extended diffuse radio emission. For the classical minimum energy estimate, such a comparison can yield constraints on the accessible parameter space spanned by lower energy cutoff of the CRe population or the contribution of CRp to the non-thermal energy density. Secondly, should the hadronic scenario be confirmed, the minimum energy estimates allow testing for the realisation of the minimum energy state for a given independent measurement of the magnetic field strength.

This article is organised as follows: After introducing synchrotron radiation of CRe (Sect. 2.1), analytic formulae for hadronically induced emission processes are presented (Sect. 2.2). The classical and hadronic minimum energy criteria are then derived, the theoretically expected tolerance regions are given, and limiting cases are discussed (Sect. 3). In Sect. 4, we examine whether future observations of inverse Compton emission and hadronically induced γ-ray emission can serve as tests for the verification of the minimum energy criterion. Magnetic and cosmic ray energy densities and their tolerance regions are inferred from application of the minimum energy arguments in the Coma and Perseus cluster for both scenarios (Sect. 5). Our article concludes with formulae which provide recipes for estimating the magnetic field strength in typical observational situations (Sect. 6). Throughout this paper we use the present Hubble constant $H_0 = 70\, h_{70}$ km s^{-1} Mpc^{-1}, where h_{70} indicates the scaling of H_0.

2 THEORETICAL BACKGROUND

This section presents our definitions and the theoretical background for this work. After introducing characteristics of the CRe population and the synchrotron emission formulae, we focus on specifications of the CRp population. Finally, the section concludes with

[1] Indeed, there are first hints for the existence of a 10 MeV - 100 MeV CRp population deriving from the detection of excited gamma-ray lines from the clusters Coma and Virgo (Iyudin et al. 2004). If verified, that would make a high energy (GeV) CRp population very plausible.

[2] Likewise the minimum energy criterion within the reacceleration scenario of mildly relativistic CRe ($\gamma_e \simeq 100 - 300$) can be obtained by minimising the sum of magnetic, mildly relativistic CRe, and turbulent energy densities while allowing for constant synchrotron emission.

analytic formulae describing the hadronically induced γ-ray and radio synchrotron emission processes.

2.1 Cosmic ray electrons and synchrotron emission

The differential number density distribution of a CRe population above a MeV is often represented by a power-law in energy E_e,

$$f_\mathrm{e}(\boldsymbol{r}, E_\mathrm{e})\,\mathrm{d}E_\mathrm{e}\,\mathrm{d}V = \tilde{n}_\mathrm{CRe}(\boldsymbol{r})\left(\frac{E_\mathrm{e}}{\mathrm{GeV}}\right)^{-\alpha_\mathrm{e}}\left(\frac{\mathrm{d}E_\mathrm{e}}{\mathrm{GeV}}\right)\mathrm{d}V. \tag{2.1}$$

where the tilde indicates that $\tilde{n}_\mathrm{CRe}$ is not a real CRe number density although it exhibits the appropriate dimensions. The normalisation $\tilde{n}_\mathrm{CRe}(\boldsymbol{r})$ might be determined by assuming that the kinetic CRe energy density $\varepsilon_\mathrm{CRe}(\boldsymbol{r})$ is expressed in terms of the thermal energy density $\varepsilon_\mathrm{th}(\boldsymbol{r})$,

$$\varepsilon_\mathrm{CRe}(\boldsymbol{r}) = X_\mathrm{CRe}(\boldsymbol{r})\,\varepsilon_\mathrm{th}(\boldsymbol{r}) = A_{E_\mathrm{e}}\,\tilde{n}_\mathrm{CRe}(\boldsymbol{r}), \tag{2.2}$$

$$A_{E_\mathrm{e}}(\alpha_\mathrm{e}) = \frac{\mathrm{GeV}}{2-\alpha_\mathrm{e}}\left[\left(\frac{E_\mathrm{e}}{\mathrm{GeV}}\right)^{2-\alpha_\mathrm{e}}\right]_{E_1}^{E_2}. \tag{2.3}$$

Here we introduced the abbreviation

$$[f(x)]_{x_1}^{x_2} = f(x_2) - f(x_1) \tag{2.4}$$

in order to account for cutoffs of the CRe population. If the CRe population had time to lose energy by means of Coulomb interactions (Gould 1972), the low energy part of the spectrum would be modified. This modification, which impacts on the CRe distribution function $f_\mathrm{e}(\boldsymbol{r}, E_\mathrm{e})$ and thus on $A_{E_\mathrm{e}}(\alpha_\mathrm{e})$, can be approximately treated by imposing a time dependent lower energy cutoff on the CRe population as described in Pfrommer & Enßlin (2004).

While the functional dependence of the CRe scaling parameter $X_\mathrm{CRe}(\boldsymbol{r})$ is a priori unknown, its radial behaviour will be adjusted such that it obeys the minimum energy criterion. The thermal energy density of the ICM ε_th is given by

$$\varepsilon_\mathrm{th}(\boldsymbol{r}) = \frac{3}{2}\,d_\mathrm{e}\,n_\mathrm{e}(\boldsymbol{r})\,kT_\mathrm{e}(\boldsymbol{r}), \tag{2.5}$$

$$\text{where}\quad d_\mathrm{e} = 1 + \frac{1-\frac{3}{4}X_\mathrm{He}}{1-\frac{1}{2}X_\mathrm{He}} \tag{2.6}$$

counts the number of particles per electron in the ICM using the primordial ^{4}He mass fraction $X_\mathrm{He} = 0.24$. T_e and n_e denote the electron temperature and number density, respectively.

The synchrotron emissivity j_ν at frequency ν and per steradian of such a CRe population (2.1), which is located in an isotropic distribution of magnetic fields (Eq. (6.36) in Rybicki & Lightman 1979), is obtained after averaging over an isotropic distribution of electron pitch angles yielding

$$j_\nu(\boldsymbol{r}) = A_{E_\mathrm{syn}}(\alpha_\mathrm{e})\,\tilde{n}_\mathrm{CRe}(\boldsymbol{r})\left[\frac{\varepsilon_B(\boldsymbol{r})}{\varepsilon_{B_\mathrm{c}}}\right]^{(\alpha_\nu+1)/2} \tag{2.7}$$

$$\propto \varepsilon_\mathrm{CRe}(\boldsymbol{r})\,B(\boldsymbol{r})^{\alpha_\nu+1}\nu^{-\alpha_\nu}, \tag{2.8}$$

$$B_\mathrm{c} = \sqrt{8\pi\,\varepsilon_{B_\mathrm{c}}} = \frac{2\pi m_\mathrm{e}^3 c^5 \nu}{3\,e\,\mathrm{GeV}^2} \simeq 31\left(\frac{\nu}{\mathrm{GHz}}\right)\,\mu\mathrm{G}, \tag{2.9}$$

$$A_{E_\mathrm{syn}} = \frac{\sqrt{3\pi}}{32\pi}\frac{B_\mathrm{c}\,e^3}{m_\mathrm{e}c^2}\frac{\alpha_\mathrm{e}+\frac{7}{3}}{\alpha_\mathrm{e}+1}\frac{\Gamma\left(\frac{3\alpha_\mathrm{e}-1}{12}\right)\Gamma\left(\frac{3\alpha_\mathrm{e}+7}{12}\right)\Gamma\left(\frac{\alpha_\mathrm{e}+5}{4}\right)}{\Gamma\left(\frac{\alpha_\mathrm{e}+7}{4}\right)}, \tag{2.10}$$

where $\Gamma(a)$ denotes the Gamma-function (Abramowitz & Stegun 1965) and $\alpha_\nu = (\alpha_\mathrm{e}-1)/2$. Note that for later convenience, we introduce a (frequency dependent) characteristic magnetic field strength B_c which implies a characteristic magnetic energy density $\varepsilon_{B_\mathrm{c}}$. Line-of-sight integration of the radio emissivity $j_\nu(\boldsymbol{r})$ yields the surface brightness of the radio emission $S_\nu(\boldsymbol{r}_\perp)$.

2.2 Cosmic ray protons

2.2.1 CRp population

In contrast to the previously introduced CRe population and owing to the higher rest mass of protons, we assume the differential number density distribution of a CRp population to be described by a power-law in momentum p_p which for instance is motivated by shock acceleration studies:

$$f_\mathrm{p}(\boldsymbol{r}, p_\mathrm{p})\,\mathrm{d}p_\mathrm{p}\,\mathrm{d}V = \tilde{n}_\mathrm{CRp}(\boldsymbol{r})\left(\frac{p_\mathrm{p}\,c}{\mathrm{GeV}}\right)^{-\alpha_\mathrm{p}}\left(\frac{c\,\mathrm{d}p_\mathrm{p}}{\mathrm{GeV}}\right)\mathrm{d}V. \tag{2.11}$$

The normalisation $\tilde{n}_\mathrm{CRp}(\boldsymbol{r})$ can be determined in such a way that the kinetic CRp energy density $\varepsilon_\mathrm{CRp}(\boldsymbol{r})$ is expressed in terms of the thermal energy density $\varepsilon_\mathrm{th}(\boldsymbol{r})$ of the ICM,

$$\varepsilon_\mathrm{CRp}(\boldsymbol{r}) = X_\mathrm{CRp}(\boldsymbol{r})\,\varepsilon_\mathrm{th}(\boldsymbol{r}) = A_{E_\mathrm{p}}\,\tilde{n}_\mathrm{CRp}(\boldsymbol{r}), \tag{2.12}$$

$$A_{E_\mathrm{p}}(\alpha_\mathrm{p}) = \frac{m_\mathrm{p}\,c^2}{2\,(\alpha_\mathrm{p}-1)}\left(\frac{m_\mathrm{p}\,c^2}{\mathrm{GeV}}\right)^{1-\alpha_\mathrm{p}}\mathcal{B}\left(\frac{\alpha_\mathrm{p}-2}{2}, \frac{3-\alpha_\mathrm{p}}{2}\right). \tag{2.13}$$

$\mathcal{B}(a, b)$ denotes the Beta-function (Abramowitz & Stegun 1965).

Aging imprints a modulation on the low energy part of the CRp spectrum by Coulomb losses in the plasma. This modification, which impacts on the CRp distribution function $f_\mathrm{p}(\boldsymbol{r}, p_\mathrm{p})$ and thus on $A_{E_\mathrm{p}}(\alpha_\mathrm{p})$, can be treated approximately by imposing a lower momentum cutoff as described in Pfrommer & Enßlin (2004). On the other side, highly energetic CRp with energies beyond 2×10^7 GeV are able to escape from the galaxy cluster assuming momentum dependent CRp diffusion in a turbulent magnetic field with a Kolmogorov-type spectrum on small scales (Berezinsky et al. 1997). The finite lifetime and size of particle accelerating shocks also give rise to high-energy breaks in the CRp spectrum. These low and high momentum cutoffs are always present in the CRp population. However, for CRp spectral indices between $2 \lesssim \alpha_\mathrm{p} \lesssim 3$ these spectral breaks have negligible influence on the CRp energy density. If the breaks are neglected, the CRp energy density would diverge for $\alpha_\mathrm{p} \lesssim 2$ at the high-energy and for $3 \lesssim \alpha_\mathrm{p}$ at the low-energy part of the spectrum. In these cases, breaks have to be included by replacing A_{E_p} in Eq. (2.12) with

$$\tilde{A}_{E_\mathrm{p}}(\alpha_\mathrm{p}) = \frac{m_\mathrm{p}\,c^2}{2\,(\alpha_\mathrm{p}-1)}\left(\frac{m_\mathrm{p}\,c^2}{\mathrm{GeV}}\right)^{1-\alpha_\mathrm{p}}\left[\mathcal{B}_{x(\tilde{p})}\left(\frac{\alpha_\mathrm{p}-2}{2}, \frac{3-\alpha_\mathrm{p}}{2}\right) + 2\,\tilde{p}^{1-\alpha_\mathrm{p}}\left(\sqrt{1+\tilde{p}^2}-1\right)\right]_{\tilde{p}_2}^{\tilde{p}_1}, \tag{2.14}$$

$$x(\tilde{p}) = (1+\tilde{p}^2)^{-1},\ \text{and}\ \tilde{p} = \frac{p_\mathrm{p}}{m_\mathrm{p}c}, \tag{2.15}$$

where $\mathcal{B}_x(a, b)$ denotes the incomplete Beta-function (Abramowitz & Stegun 1965) and $\tilde{p}_1$ and $\tilde{p}_2$ are the lower and higher break momenta, respectively.

2.2.2 Hadronically induced γ-ray emission

The CRp interact hadronically with the ambient thermal gas and produce pions, provided their momentum exceeds the kinematic threshold $p_\mathrm{thr} = 0.78\ \mathrm{GeV}\,c^{-1}$ for the reaction. The neutral pions decay into γ-rays while the charged pions decay into secondary electrons (and neutrinos):

$$\pi^\pm \rightarrow \mu^\pm + \nu_\mu/\overline{\nu}_\mu \rightarrow e^\pm + \nu_e/\overline{\nu}_e + \nu_\mu + \overline{\nu}_\mu$$
$$\pi^0 \rightarrow 2\gamma\,.$$

Only the CRp population above the kinematic threshold p_thr is visible through its decay products in γ-ray and synchrotron emission.

An analytic formula describing the omnidirectional (i.e. integrated over 4π solid angle) differential γ-ray source function resulting from π^0-decay of a power-law CRp population is given in Pfrommer & Enßlin (2004):

$$q_\gamma(\boldsymbol{r}, E_\gamma)\,\mathrm{d}E_\gamma\,\mathrm{d}V \simeq \sigma_{\mathrm{pp}}\, c\, n_{\mathrm{N}}(\boldsymbol{r})\, 2^{2-\alpha_\gamma}\, \frac{\tilde{n}_{\mathrm{CRp}}(\boldsymbol{r})}{\mathrm{GeV}} \times \frac{4}{3\,\alpha_\gamma} \left(\frac{m_{\pi^0}\,c^2}{\mathrm{GeV}}\right)^{-\alpha_\gamma} \left[\left(\frac{2\,E_\gamma}{m_{\pi^0}\,c^2}\right)^{\delta_\gamma} + \left(\frac{2\,E_\gamma}{m_{\pi^0}\,c^2}\right)^{-\delta_\gamma}\right]^{-\alpha_\gamma/\delta_\gamma} \mathrm{d}E_\gamma\,\mathrm{d}V, \tag{2.16}$$

where $n_{\mathrm{N}}(\boldsymbol{r}) = d_{\mathrm{tar}}\, n_{\mathrm{e}}(\boldsymbol{r}) = n_{\mathrm{e}}(\boldsymbol{r})/(1 - \frac{1}{2}X_{\mathrm{He}})$ denotes the target nucleon density in the ICM while assuming primordial element composition with $X_{\mathrm{He}} = 0.24$, which holds approximately. The formalism also includes the detailed physical processes at the threshold of pion production like the velocity distribution of CRp, momentum dependent inelastic CRp-p cross section, and kaon decay channels. The shape parameter δ_γ and the effective cross section σ_{pp} depend on the spectral index of the γ-ray spectrum α_γ according to

$$\delta_\gamma \simeq 0.14\,\alpha_\gamma^{-1.6} + 0.44 \quad \text{and} \tag{2.17}$$

$$\sigma_{\mathrm{pp}} \simeq 32 \cdot \left(0.96 + \mathrm{e}^{4.4 - 2.4\,\alpha_\gamma}\right)\ \mathrm{mbarn}. \tag{2.18}$$

There is a detailed discussion in Pfrommer & Enßlin (2004) how the γ-ray spectral index α_γ relates to the spectral index of the parent CRp population α_{p}. In Dermer's model, which is motivated by accelerator experiments, the pion multiplicity is independent of energy yielding the relation $\alpha_\gamma = \alpha_{\mathrm{p}}$ (Dermer 1986a,b).

Provided the CRp population has a power-law spectrum, the integrated γ-ray source density λ_γ for pion decay induced γ-rays can be obtained by integrating the γ-ray source function $q_\gamma(\boldsymbol{r}, E_\gamma)$ in Eq. (2.16) over an energy interval yielding

$$\lambda_\gamma(\boldsymbol{r}, E_1, E_2) = \int_{E_1}^{E_2} \mathrm{d}E_\gamma\, q_\gamma(\boldsymbol{r}, E_\gamma) \tag{2.19}$$

$$= A_\gamma(\alpha_{\mathrm{p}})\, A_{E_{\mathrm{p}}}^{-1}(\alpha_{\mathrm{p}})\, X_{\mathrm{CRp}}(\boldsymbol{r})\, n_{\mathrm{e}}^2(\boldsymbol{r})\, kT_{\mathrm{e}}(\boldsymbol{r}), \tag{2.20}$$

$$\text{where } A_\gamma(\alpha_{\mathrm{p}}) = \frac{\sigma_{\mathrm{pp}}(\alpha_{\mathrm{p}})\, c\, d_{\mathrm{e}}\, d_{\mathrm{tar}} \left[\mathcal{B}_x\left(\frac{\alpha_\gamma+1}{2\,\delta_\gamma}, \frac{\alpha_\gamma-1}{2\,\delta_\gamma}\right)\right]_{x_1}^{x_2}}{\left(\frac{m_{\pi^0}\,c^2}{\mathrm{GeV}}\right)^{\alpha_\gamma-1} 2^{\alpha_\gamma-1}\,\alpha_\gamma\,\delta_\gamma}, \tag{2.21}$$

$$\text{and } x_i = \left[1 + \left(\frac{m_{\pi^0}\,c^2}{2\,E_i}\right)^{2\delta_\gamma}\right]^{-1} \text{ for } i \in \{1, 2\}. \tag{2.22}$$

The γ-ray number flux $\mathcal{F}_\gamma$ is derived by means of volume integration over the emission region and correct accounting for the growth of the area of the emission sphere on which the photons are distributed:

$$\mathcal{F}_\gamma(E_1, E_2) = \frac{1+z}{4\pi D^2} \int \mathrm{d}V\, \lambda_\gamma[\boldsymbol{r}, (1+z)E_1, (1+z)E_2]. \tag{2.23}$$

Here D denotes the luminosity distance and the additional factors of $1 + z$ account for the cosmological redshift of the photons.

2.2.3 Hadronically induced synchrotron emission

Following for instance Dolag & Enßlin (2000) and Pfrommer & Enßlin (2004), the steady-state CRe spectrum is governed by injection of secondaries and cooling processes so that it can be described by the continuity equation

$$\frac{\partial}{\partial E_{\mathrm{e}}}\left(\dot{E}_{\mathrm{e}}(\boldsymbol{r}, E_{\mathrm{e}}) f_{\mathrm{e}}(\boldsymbol{r}, E_{\mathrm{e}})\right) = q_{\mathrm{e}}(\boldsymbol{r}, E_{\mathrm{e}})\,. \tag{2.24}$$

For $\dot{E}_{\mathrm{e}}(\boldsymbol{r}, p) < 0$ this equation is solved by

$$f_{\mathrm{e}}(\boldsymbol{r}, E_{\mathrm{e}}) = \frac{1}{|\dot{E}_{\mathrm{e}}(\boldsymbol{r}, E_{\mathrm{e}})|} \int_{E_{\mathrm{e}}}^{\infty} \mathrm{d}E'_{\mathrm{e}}\, q_{\mathrm{e}}(\boldsymbol{r}, E'_{\mathrm{e}})\,. \tag{2.25}$$

For the energy range of interest, the cooling of the radio emitting CRe is dominated by synchrotron and inverse Compton losses:

$$-\dot{E}_{\mathrm{e}}(\boldsymbol{r}, E_{\mathrm{e}}) = \frac{4\,\sigma_{\mathrm{T}}\,c}{3\,m_{\mathrm{e}}^2\,c^4}\,[\varepsilon_B(\boldsymbol{r}) + \varepsilon_{\mathrm{CMB}}]\; E_{\mathrm{e}}^2\,, \tag{2.26}$$

where σ_{T} is the Thomson cross section, $\varepsilon_B(\boldsymbol{r})$ is the local magnetic field energy density, and $\varepsilon_{\mathrm{CMB}} = B_{\mathrm{CMB}}^2/(8\pi)$ is the energy density of the cosmic microwave background expressed by an equivalent field strength $B_{\mathrm{CMB}} = 3.24\,(1+z)^2\,\mu\mathrm{G}$. Assuming that the parent CRp population is represented by a power-law (2.11), the CRe population above a GeV is therefore described by a power-law spectrum

$$f_{\mathrm{e}}(\boldsymbol{r}, E_{\mathrm{e}}) = \frac{\tilde{n}_{\mathrm{CRe}}(\boldsymbol{r})}{\mathrm{GeV}} \left(\frac{E_{\mathrm{e}}}{\mathrm{GeV}}\right)^{-\alpha_{\mathrm{e}}}, \tag{2.27}$$

$$\text{and } \tilde{n}_{\mathrm{CRe}}(\boldsymbol{r}) = A_{\varepsilon_{\mathrm{eff}}}(\boldsymbol{r})\, \frac{\tilde{n}_{\mathrm{CRp}}(\boldsymbol{r})}{\varepsilon_B(\boldsymbol{r}) + \varepsilon_{\mathrm{CMB}}}, \tag{2.28}$$

$$A_{\varepsilon_{\mathrm{eff}}}(\boldsymbol{r}) = \frac{16^{-(\alpha_{\mathrm{e}}-2)}}{\alpha_{\mathrm{e}} - 2}\, \frac{\sigma_{\mathrm{pp}}\, m_{\mathrm{e}}^2\, c^4\, n_{\mathrm{N}}(\boldsymbol{r})}{\sigma_{\mathrm{T}}\,\mathrm{GeV}}, \tag{2.29}$$

where the effective CRp-p cross section σ_{pp} is given by Eq. (2.18).

The hadronically induced synchrotron emissivity j_ν at frequency ν and per steradian of such a CRe population (2.27) which is located in an isotropic distribution of magnetic fields within the halo volume is given by Eq. (2.7). However, the normalisation $\tilde{n}_{\mathrm{CRe}}(\boldsymbol{r})$ of the CRe population is given by Eq. (2.28). The spectral index of the synchrotron emission is related to the CRp spectral index by $\alpha_\nu = (\alpha_{\mathrm{e}} - 1)/2 = \alpha_{\mathrm{p}}/2$.

3 MINIMUM ENERGY CRITERIA

This section develops minimum energy criteria in order to estimate the magnetic field and studies the tolerance region of the obtained estimates. As described in Sect. 1, we discuss two different approaches when requiring the non-thermal energy density of the source to be minimal for a particular (observed) synchrotron emission. The classical minimum energy criterion used in radio astronomy (Pohl 1993; Beck et al. 1996; Brunetti et al. 1997) can be applied irrespective of the particular acceleration process of CRe, but unfortunately it relies on uncertain assumptions or parameters. Provided the hadronic scenario of synchrotron emission applies, these dependencies can be softened. The resulting minimum energy argument needs to be changed accordingly.

The philosophy of these approaches is to provide an estimate of the energetically least expensive radio emission model possible in each of these physically motivated scenarios. Thus, the obtained minimum energy estimates should not be taken literally in a sense that they are necessarily realised in Nature. However, the minimum energy estimates allow scrutinising the hadronic model for extended radio synchrotron emission in clusters of galaxies by comparing to the thermal energy density. For the classical minimum energy estimate, such a comparison can yield important constraints on the accessible parameter space.

The non-thermal energy density in the intra-cluster medium (ICM), which is the quantity to be minimised, is composed of the sum of the energy densities in magnetic fields, CRp and CRe:

$$\varepsilon_{\mathrm{NT}} = \varepsilon_B + \varepsilon_{\mathrm{CRp}} + \varepsilon_{\mathrm{CRe}}. \tag{3.1}$$

The CRp population also includes higher mass nuclei in addition to protons. For convenience, we introduce canonical dimensionless

energy densities by means of scaling with the critical magnetic energy density $\varepsilon_{B_\mathrm{c}} = B_\mathrm{c}^2/(8\pi)$, where B_c is defined in Eq. (2.9):

$$x_\mathrm{NT}(\boldsymbol{r}) \equiv \frac{\varepsilon_\mathrm{NT}(\boldsymbol{r})}{\varepsilon_{B_\mathrm{c}}}\,,\; x_\mathrm{CRp}(\boldsymbol{r}) \equiv \frac{\varepsilon_\mathrm{CRp}(\boldsymbol{r})}{\varepsilon_{B_\mathrm{c}}}\,,\; x_\mathrm{CRe}(\boldsymbol{r}) \equiv \frac{\varepsilon_\mathrm{CRe}(\boldsymbol{r})}{\varepsilon_{B_\mathrm{c}}}\,, \tag{3.2}$$

$$x_B(\boldsymbol{r}) \equiv \frac{\varepsilon_B(\boldsymbol{r})}{\varepsilon_{B_\mathrm{c}}}\,,\; x_\mathrm{th}(\boldsymbol{r}) \equiv \frac{\varepsilon_\mathrm{th}(\boldsymbol{r})}{\varepsilon_{B_\mathrm{c}}}\,,\; \text{and } x_\mathrm{CMB} \equiv \frac{\varepsilon_\mathrm{CMB}}{\varepsilon_{B_\mathrm{c}}}\,. \tag{3.3}$$

After presenting the conceptually simpler classical minimum energy criterion, we will subsequently discuss the hadronic minimum energy criterion.

3.1 Classical minimum energy criterion

This section presents the classical minimum energy criterion from a physically motivated point of view, probing synchrotron emission from CRe characterised by a power-law distribution function without specifying their origin. This approach implies putting up with a dependence of the inferred magnetic field strength on unknown parameters like the lower energy cutoff of the CRe population or the unknown contribution of CRp to the non-thermal energy density.

3.1.1 Derivation

Assuming a proportionality between the CRe and CRp energy densities, i.e. $x_\mathrm{CRp} = k_\mathrm{p} x_\mathrm{CRe}$, the non-thermal energy composition equation (3.1) can be written as

$$x_\mathrm{NT} = x_B + (1 + k_\mathrm{p}) x_\mathrm{CRe}. \tag{3.4}$$

This assumption is reasonable if for instance the thermal electron population and the CRp were energised by the same shock wave assuming that there is a constant fraction of energy going into the CRp population by such an acceleration process, provided injection processes alone determine the energies. In order to proceed, we need an expression for j_ν (given by Eq. (2.7)) as a function of the dimensionless energy densities considered here:

$$j_\nu(\boldsymbol{r}) = \frac{A_{E_\mathrm{syn}}(\alpha_\mathrm{e})\,\varepsilon_{B_\mathrm{c}}}{A_{E_\mathrm{e}}}\, x_\mathrm{CRe}(\boldsymbol{r})\, x_B(\boldsymbol{r})^{1+\delta}, \quad \text{where} \tag{3.5}$$

$$\delta = \frac{\alpha_\nu - 1}{2} = \frac{\alpha_\mathrm{e} - 3}{4}. \tag{3.6}$$

For consistency reasons, which will become clear in Sect. 3.2, we introduce δ as a parametrisation of the spectral index. For typical radio (mini-)halos, δ is a small quantity: The synchrotron spectral index $\alpha_\nu = 1$ corresponds to $\delta = 0$. Solving Eq. (3.5) for the CRe energy density yields

$$x_\mathrm{CRe} = C_\mathrm{class}(\boldsymbol{r})\, x_B(\boldsymbol{r})^{-1-\delta}, \quad \text{where} \tag{3.7}$$

$$C_\mathrm{class}(\boldsymbol{r}) \equiv \frac{A_{E_\mathrm{e}}\, j_\nu(\boldsymbol{r})}{A_{E_\mathrm{syn}}\, \varepsilon_{B_\mathrm{c}}} \propto \frac{j_\nu}{\nu^3} \tag{3.8}$$

is a convenient auxiliary variable. Combining Eqs. (3.4) and (3.7) yields the non-thermal energy density solely as a function of the magnetic energy density

$$x_\mathrm{NT} = x_B + (1 + k_\mathrm{p})\, C_\mathrm{class}(\boldsymbol{r})\, x_B(\boldsymbol{r})^{-1-\delta}. \tag{3.9}$$

Requesting this energy density to be minimal for a given synchrotron emissivity yields the energetically least expensive radio emission model possible in this approach:

$$\left(\left.\frac{\partial x_\mathrm{NT}}{\partial x_B}\right|_{j_\nu}\right) = 1 - (1 + k_\mathrm{p})(1 + \delta)\, C_\mathrm{class}(\boldsymbol{r}) x_B(\boldsymbol{r})^{-2-\delta} \stackrel{!}{=} 0. \tag{3.10}$$

The corresponding CRp, CRe and magnetic energy densities are given by

$$x_{B_\mathrm{min}}(\boldsymbol{r}) = \left[(1 + k_\mathrm{p})(1 + \delta)\, C_\mathrm{class}(\boldsymbol{r})\right]^{1/(2+\delta)}, \tag{3.11}$$

$$x_{\mathrm{CRe}_\mathrm{min}}(\boldsymbol{r}) = C_\mathrm{class}(\boldsymbol{r}) \left[(1 + k_\mathrm{p})(1 + \delta)\, C_\mathrm{class}(\boldsymbol{r})\right]^{-(1+\delta)/(2+\delta)}, \tag{3.12}$$

$$x_{\mathrm{CRp}_\mathrm{min}}(\boldsymbol{r}) = k_\mathrm{p}\, x_{\mathrm{CRe}_\mathrm{min}}(\boldsymbol{r}). \tag{3.13}$$

Note that these formulae deviate from Pacholczyk (1970), since we use a fixed interval in CRe energy rather than in radio frequency (c.f. Sect. 1). However, they are equivalent to those obtained by Brunetti et al. (1997).

3.1.2 Localisation of classical minimum energy densities

We wish to quantify how tight our statements about the inferred minimum energy densities are, i.e. to assign a tolerance region to the minimum energy estimates. This region would have the meaning of a quasi-optimal realisation of the particular energy densities. The curvature radius at the extremal value is one possible way of characterising the 'sharpness' of the minimum:[3]

$$\sigma_{x_B,\mathrm{Gauss}} \equiv \left(\left.\frac{1}{x_\mathrm{NT}} \frac{\partial^2 x_\mathrm{NT}}{\partial x_B^2}\right|_{x_{B_\mathrm{min}}}\right)^{-1/2}. \tag{3.14}$$

In order to avoid unphysical negative values for the lower tolerance level of x_{B_min} we rather adopt the following logarithmic measure of the curvature:

$$\sigma_{\ln x_B} \equiv \left(\left.\frac{\partial^2 \ln x_\mathrm{NT}}{\partial (\ln x_B)^2}\right|_{x_{B_\mathrm{min}}}\right)^{-1/2}. \tag{3.15}$$

Considering the linear representation of x_B, this definition explicitly implies tolerance levels which are given by $\exp(\ln x_B \pm \sigma_{\ln x_B})$. Applying this definition to Eq. (3.9) yields the theoretical tolerance level of the estimated minimum magnetic energy density,

$$\sigma_{\ln x_B}(\boldsymbol{r}) = \left\{\frac{x_{B_\mathrm{min}}^{-2-\delta}\left[C_\mathrm{class}\left(1 + k_\mathrm{p}\right) + x_{B_\mathrm{min}}^{2+\delta}\right]^2}{C_\mathrm{class}\left(1 + k_\mathrm{p}\right)(2 + \delta)^2}\right\}^{1/2}(\boldsymbol{r}). \tag{3.16}$$

The tolerance level of the estimated minimum CRp energy density is given by

$$\sigma_{\ln x_\mathrm{CRp}} \equiv \left|\left.\frac{\partial \ln x_\mathrm{CRp}}{\partial \ln x_B}\right|_{x_{B_\mathrm{min}}}\right| \sigma_{\ln x_B}, \tag{3.17}$$

while the theoretical tolerance level of the estimated minimum CRe energy density can be obtained likewise. Applying this Gaussian error propagation to Eq. (3.7), we obtain following general result:

$$\sigma_{\ln x_\mathrm{CRp}} = \sigma_{\ln x_\mathrm{CRe}} = (1 + \delta)\, \sigma_{\ln x_B}. \tag{3.18}$$

3.1.3 Equipartition condition

In order to investigate under which conditions the classical minimum energy criterion implies exact equipartition, we examine the

[3] One could picture this approach by assuming Gaussian statistics for the distribution of non-thermal energy densities. The curvature radius at the minimum would then correspond to the width σ_B and thus yielding the 68%-confidence level with respect to this extremal value.

special case $\delta = 0$ of Eq. (3.11). The resulting minimal magnetic and CRp energy densities read

$$x_{B_{0,\min}}(\boldsymbol{r}) = \sqrt{(1+k_\mathrm{p})\, C_\mathrm{class}(\boldsymbol{r})}\,, \tag{3.19}$$

$$x_{\mathrm{CRp}_{0,\min}}(\boldsymbol{r}) = \sqrt{\frac{k_\mathrm{p}^2\, C_\mathrm{class}(\boldsymbol{r})}{(1+k_\mathrm{p})}} \stackrel{k_\mathrm{p}\gg 1}{\longrightarrow} x_{B_{0,\min}}(\boldsymbol{r})\,. \tag{3.20}$$

This comparison shows that there exists exact equipartition between the CRp and magnetic energy densities if $\delta = 0$ and $k_\mathrm{p} \gg 1$! In our Galaxy $k_\mathrm{p} \simeq 100$ (Beck et al. 1996) and $\alpha_\nu = \alpha_\mathrm{GHz} = 0.8$ suggesting $\delta = -0.1$ (Beuermann et al. 1985), which implies that these equipartition conditions are well fulfilled. When comparing to a combination of synchrotron emission, the local CRe density, and diffuse continuum γ-rays, Strong et al. (2000) interestingly imply the same magnetic field strength as inferred from equipartition arguments (Beck et al. 1996). The corresponding minimal CRe energy density is given by

$$x_{\mathrm{CRe}_{0,\min}}(\boldsymbol{r}) = \sqrt{\frac{C_\mathrm{class}(\boldsymbol{r})}{(1+k_\mathrm{p})}} \stackrel{k_\mathrm{p}\ll 1}{\longrightarrow} x_{B_{0,\min}}(\boldsymbol{r})\,. \tag{3.21}$$

The classical minimum energy densities in CRe and magnetic fields are in exact equipartition if $\delta = 0$ and $k_\mathrm{p} \ll 1$! In the limiting case $\delta = 0$, the theoretical tolerance levels of the estimated classical minimum energy densities read

$$\sigma_{\ln x_{B_0}} = \sigma_{\ln x_{\mathrm{CRp}_0}} = \sigma_{\ln x_{\mathrm{CRe}_0}} = 1. \tag{3.22}$$

3.2 Hadronic minimum energy criterion

This section deals with the hadronic minimum energy criterion and thus probes hadronically induced synchrotron emission. If a significant part of the CRe population is known to be generated by hadronic interactions, the minimum energy estimate allows testing for the realisation of the minimum energy state for a given independent measurement of the magnetic field strength. Thus, the proposed minimum energy criterion would provide information about the dynamical state of the magnetic field.

3.2.1 Derivation

To derive the hadronic minimum energy criterion, we need an expression for the CRp energy density as a function of the magnetic energy density which is obtained by combining Eqs. (2.7) and (2.28):

$$x_\mathrm{CRp}(\boldsymbol{r}) = C_\mathrm{hadr}(\boldsymbol{r})\,[x_B(\boldsymbol{r}) + x_\mathrm{CMB}]\, x_B(\boldsymbol{r})^{-1-\delta}, \tag{3.23}$$

$$C_\mathrm{hadr}(\boldsymbol{r}) \equiv \frac{A_{E_\mathrm{p}}}{A_{E_\mathrm{syn}}} \frac{j_\nu(\boldsymbol{r})}{A_{\varepsilon_\mathrm{eff}}(\boldsymbol{r})} \propto \frac{j_\nu(\boldsymbol{r})}{\nu\, n_\mathrm{N}(\boldsymbol{r})}, \tag{3.24}$$

$$\delta = \frac{\alpha_\nu - 1}{2} = \frac{\alpha_\mathrm{e} - 3}{4} = \frac{\alpha_\mathrm{p} - 2}{4}. \tag{3.25}$$

The parameter $C_\mathrm{hadr}(\boldsymbol{r})$ has the meaning of a hadronic synchrotron emissivity per target nucleon density and per frequency. Its value decreases for any existing cutoff in the parent CRp population as described by Eq. (2.14). For convenience we introduce the parameter δ which ranges within $[-0.1, 0.2]$ for conceivable CRp spectral indices $\alpha_\mathrm{p} = [1.6, 2.8]$.

Assuming the hadronic electron source to be dominant, we can neglect the primary CRe population. In any case, the energy density of hadronically generated CRe is negligible compared to the energy density of the parent CRp population: Above energies of $\sim$ GeV the differential hadronic $\tilde{k}_\mathrm{p} = \tilde{n}_\mathrm{CRp}/\tilde{n}_\mathrm{CRe}$ has typically values ranging between $\tilde{k}_\mathrm{p} \sim 100$ (Perseus) and $\tilde{k}_\mathrm{p} \sim 300$ (Coma), where we inserted the typical values of the central density and magnetic field strength. The tilde in $\tilde{k}_\mathrm{p}$ indicates the slightly modified definition compared to the previous classical case. Requiring minimum non-thermal energy density within the hadronic framework for a given synchrotron emissivity yields

$$\left(\left.\frac{\partial x_\mathrm{NT}}{\partial x_B}\right|_{j_\nu}\right) = 1 + \left.\frac{\partial x_\mathrm{CRp}}{\partial x_B}\right|_{j_\nu} \stackrel{!}{=} 0. \tag{3.26}$$

By using Eq. (3.23) we obtain the following implicit equation for the minimum magnetic energy density:

$$\left[(1+\delta)\, x_\mathrm{CMB} + \delta x_{B_\mathrm{min}}(\boldsymbol{r})\right]\, x_{B_\mathrm{min}}(\boldsymbol{r})^{-2-\delta} = C_\mathrm{hadr}^{-1}(\boldsymbol{r}). \tag{3.27}$$

The definition of $C_\mathrm{hadr}(\boldsymbol{r})$ (3.24) reveals an implicit dependence on the parametrised spectral index δ. However, the right hand side of the minimum energy criterion (3.27) is uniquely determined for a given spectral index and an observed synchrotron emissivity at a particular frequency. Thus, the minimum energy density of the magnetic field giving rise to an observed synchrotron emission in the hadronic model can either be obtained by solving Eq. (3.27) numerically or applying the asymptotic expansion which will be developed in Sect. 3.2.2.

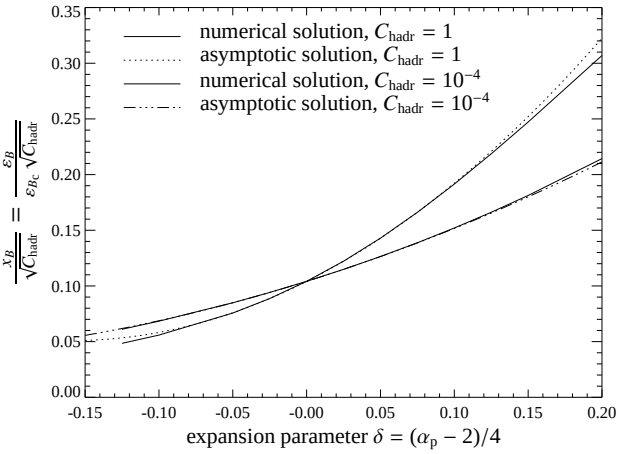

Figure 1. Comparison between the numerical solution and the second order asymptotic expansion for $C_\mathrm{hadr} = 1$ (cool core cluster, formerly referred to as cooling flow cluster) and $C_\mathrm{hadr} = 10^{-4}$ (cluster without a cool core). The perfect match indicates a fast convergence of the asymptotic solution for the range of δ being considered.

3.2.2 Asymptotic expansion for $\delta \neq 0$

The asymptotic expansion of the magnetic field energy density as a function of the small parameter δ follows from the minimum energy criterion (3.27):

$$x_{B_\mathrm{min}}(\boldsymbol{r}) = x_{B_0}(\boldsymbol{r}) + \delta x_{B_1}(\boldsymbol{r}) + \delta^2 x_{B_2}(\boldsymbol{r}) + O(\delta^3), \tag{3.28}$$

$$x_{B_0}(\boldsymbol{r}) = \sqrt{C_\mathrm{hadr}(\boldsymbol{r})\, x_\mathrm{CMB}}, \tag{3.29}$$

$$x_{B_1}(\boldsymbol{r}) = \frac{x_{B_0}}{2}\left(1 - \ln x_{B_0} + \frac{x_{B_0}}{x_\mathrm{CMB}}\right)(\boldsymbol{r}), \tag{3.30}$$

$$x_{B_2}(\boldsymbol{r}) = \frac{x_{B_0}}{2}\left[-\frac{1}{2}\left(\ln x_{B_0}\right)^2 - \frac{x_{B_1}}{x_{B_0}}\left(2 + \ln x_{B_0}\right) + \frac{x_{B_1}^2}{x_{B_0}^2}\right]. \tag{3.31}$$

A comparison between the numerical solution and the asymptotic solution for two different values of the parameter C_hadr is shown

in Fig. 1. The particular values of the parameter $C_{\rm hadr}$ will be motivated in Sect. 5.2. This figure should serve as mathematical illustration of the convergence behaviour of the asymptotic expansion while keeping the parameter $C_{\rm hadr}$ fixed. The second order asymptotic solution perfectly agrees with the exact solution for the range $\delta = [-0.15, 0.2]$ of conceivable CRp spectral indices $\alpha_{\rm p} = [1.6, 2.8]$.

3.2.3 Localisation of hadronic minimum energy densities

Considering the accuracy of the estimated minimum energy densities in the hadronic scenario, we can also apply the logarithmic measure of the theoretical tolerance level as defined in Eq. (3.15):

$$\sigma_{\ln x_B}(\boldsymbol{r}) = \left[x_{B_{\rm min}}^{2+\delta} + C_{\rm hadr}\left(x_{B_{\rm min}} + x_{\rm CMB}\right)\right](C_{\rm hadr}\, x_{B_{\rm min}})^{-1/2} \times \left\{C_{\rm hadr}\, x_{\rm CMB} + x_{B_{\rm min}}^{1+\delta}\left[(1+\delta)^2 x_{B_{\rm min}} + (2+\delta)^2 x_{\rm CMB}\right]\right\}^{-1/2}(\boldsymbol{r}). \quad (3.32)$$

The corresponding tolerance level for the minimum CRp energy density is obtained by applying Gaussian error propagation (3.17):

$$\sigma_{\ln x_{\rm CRp}}(\boldsymbol{r}) = \left(\frac{x_{\rm CMB}}{x_{B_{\rm min}}(\boldsymbol{r}) + x_{\rm CMB}} + \delta\right)\sigma_{\ln x_B}(\boldsymbol{r}). \quad (3.33)$$

The consequences of these rather unwieldy formulae will become intuitively clear in the next section where characteristic limiting cases are investigated.

3.2.4 Special cases

In order to gain insight into the hadronic minimum energy criterion, we investigate special cases of Eq. (3.27), namely $\delta \to 0$, $\varepsilon_B \gg \varepsilon_{\rm CMB}$, and $\varepsilon_B \ll \varepsilon_{\rm CMB}$, while simultaneously considering the resulting tolerance regions of the previous Sect. 3.2.3.

(i) $\delta \to 0$: The limit of $\delta \to 0$ corresponds to a hard spectral CRp population described by a spectral index of $\alpha_{\rm p} = 2.0$ and thus $\alpha_\nu = 1$. There the dimensionless magnetic field energy density reads

$$x_{B_{0,\rm min}}(\boldsymbol{r}) = \sqrt{C_{\rm hadr}(\boldsymbol{r})\, x_{\rm CMB}} \propto \left[\frac{j_\nu(\boldsymbol{r})\,\varepsilon_{\rm CMB}}{\nu\, n_{\rm N}(\boldsymbol{r})}\right]^{1/2}. \quad (3.34)$$

We can formulate the corresponding dimensionless CRp energy density resulting from this minimising argument:

$$x_{{\rm CRp}_{0,\rm min}}(\boldsymbol{r}) = C_{\rm hadr}(\boldsymbol{r}) + \sqrt{C_{\rm hadr}(\boldsymbol{r})\, x_{\rm CMB}}. \quad (3.35)$$

It is interesting to note that there are two regimes for $x_{{\rm CRp}_{0,\rm min}}$, namely

$$x_{{\rm CRp}_{0,\rm min}}(\boldsymbol{r}) = \begin{cases} C_{\rm hadr}(\boldsymbol{r}), & \text{for } C_{\rm hadr}(\boldsymbol{r}) \gg 0.01\,\nu_{\rm GHz}^{-2}, \\ x_{B_{0,\rm min}}(\boldsymbol{r}), & \text{for } C_{\rm hadr}(\boldsymbol{r}) \ll 0.01\,\nu_{\rm GHz}^{-2}. \end{cases} \quad (3.36)$$

Only in the limit of a small parameter $C_{\rm hadr}(\boldsymbol{r})$ and $\delta = 0$, there is an exact equipartition between the hadronic minimum energy densities in CRp and magnetic fields!

The tolerance regions of the estimated minimum energy densities are also more intuitive to understand in the limit $\delta = 0$ compared to the general case laid down in Eq. (3.32):

$$\sigma_{\ln x_{B_0}}(\boldsymbol{r}) = \left(1 + \frac{x_{B_{0,\rm min}}(\boldsymbol{r})}{2x_{\rm CMB}}\right)^{1/2}, \quad \text{implying two regimes:}$$

$$\sigma_{\ln x_{B_0}}(\boldsymbol{r}) = \begin{cases} 1, & \text{for } x_{B_{0,\rm min}} \ll x_{\rm CMB}, \\ \left[\frac{x_{B_{0,\rm min}}(\boldsymbol{r})}{2x_{\rm CMB}}\right]^{1/2}, & \text{for } x_{B_{0,\rm min}} \gg x_{\rm CMB}. \end{cases} \quad (3.37)$$

In the previously studied classical case (3.22), the tolerance region remains constant for all conceivable magnetic energy densities. In contrast to this, the hadronic scenario shows a increasing tolerance region $\sigma_{\ln x_{B_0}}$ for strong magnetic field strengths ($B_{0,\rm min} \gg 3.24\,(1+z)^2$ μG) which is explained by the following argument: In the limit of strong magnetic fields, the hadronically induced synchrotron emission with $\alpha_\nu = 1$ does not depend any more on the magnetic field strength but only on the CRp energy density. This is, because the inverse Compton cooling is negligible in this regime, implying that observed synchrotron emission is insensitive to any variation of the magnetic field strength since all injected CRe energy results in synchrotron emission. Therefore magnetic field estimates inferred from minimum energy arguments are rather uncertain in the limit of strong magnetic field strengths.

The tolerance levels of the corresponding CRp energy density, derived from Eq. (3.33), shows two limiting regimes:

$$\sigma_{\ln x_{{\rm CRp}_0}}(\boldsymbol{r}) = \left(1 + \frac{x_{B_{0,\rm min}}(\boldsymbol{r})}{x_{\rm CMB}}\right)^{-1}\left(1 + \frac{x_{B_{0,\rm min}}(\boldsymbol{r})}{2x_{\rm CMB}}\right)^{1/2}, \text{ implying}$$

$$\sigma_{\ln x_{{\rm CRp}_0}}(\boldsymbol{r}) = \begin{cases} 1, & \text{for } x_{B_{0,\rm min}} \ll x_{\rm CMB}, \\ \left[\frac{x_{\rm CMB}}{x_{B_{0,\rm min}}(\boldsymbol{r})}\right]^{1/2}, & \text{for } x_{B_{0,\rm min}} \gg x_{\rm CMB}. \end{cases} \quad (3.38)$$

The tolerance region of the inferred minimum CRp energy density decreases in the regime of strong magnetic fields which can be understood by the same token as above, i.e. synchrotron losses dominate over the inverse Compton cooling in this limit. Thus, the observed radio emission reflects accurately the CRp energy density in the strong magnetic field limit.

(ii) $\varepsilon_B \gg \varepsilon_{\rm CMB}$: In the limit of $\varepsilon_B \gg \varepsilon_{\rm CMB}$, the magnetic field energy density is an even stronger function of the synchrotron emissivity and the number density of the ambient gas:

$$x_{B_{\rm min}}(\boldsymbol{r}) = [\delta\, C_{\rm hadr}(\boldsymbol{r})]^{1/(1+\delta)} \quad (3.39a)$$

$$\simeq \delta\, C_{\rm hadr}(\boldsymbol{r})^{1/(1+\delta)} \propto \delta\left[\frac{j_\nu(\boldsymbol{r})}{\nu\, n_{\rm N}(\boldsymbol{r})}\right]^{1/(1+\delta)}, \quad (3.39b)$$

where we assumed $|\delta| \ll 1$ in the second step. In the limit of strong magnetic fields and small δ, exact equipartition of the magnetic and CRp hadronic minimum energy density does not occur, because

$$x_{{\rm CRp}_{\rm min}}(\boldsymbol{r}) = \delta^{-\delta/(1+\delta)} C_{\rm hadr}(\boldsymbol{r})^{1/(1+\delta)} \simeq C_{\rm hadr}(\boldsymbol{r})^{1/(1+\delta)}(1 - \delta\,\ln\delta). \quad (3.40)$$

(iii) $\varepsilon_{\rm CMB} \gg \varepsilon_B$: In the opposite limit, we obtain the following minimum energy criterion for the magnetic field energy density:

$$x_{B_{\rm min}}(\boldsymbol{r}) = [(1+\delta)\, x_{\rm CMB}\, C_{\rm hadr}(\boldsymbol{r})]^{1/(2+\delta)} \quad (3.41a)$$

$$\simeq \left(1 + \frac{\delta}{2}\right)[x_{\rm CMB} C_{\rm hadr}(\boldsymbol{r})]^{1/(2+\delta)} \quad (3.41b)$$

$$\propto \left(1 + \frac{\delta}{2}\right)\left[\frac{j_\nu(\boldsymbol{r})\varepsilon_{\rm CMB}}{\nu\, n_{\rm N}(\boldsymbol{r})}\right]^{1/(2+\delta)}, \quad (3.41c)$$

where we again assumed $\delta \ll 1$ in the second step. In contrast to the previous limit, there is exact equipartition between the magnetic and CRp hadronic minimum energy density to zeroth order in δ,

$$x_{{\rm CRp}_{\rm min}}(\boldsymbol{r}) = (1+\delta)^{-(1+\delta)/(2+\delta)}\,[x_{\rm CMB} C_{\rm hadr}(\boldsymbol{r})]^{1/(2+\delta)} \quad (3.42a)$$

$$\simeq \left(1 - \frac{\delta}{2}\right)[x_{\rm CMB} C_{\rm hadr}(\boldsymbol{r})]^{1/(2+\delta)}. \quad (3.42b)$$

4 FUTURE TESTING

This section will discuss possibilities of measuring the magnetic field strength, averaged over the cluster volume, in order to test for

the realisation of the energetically least expensive state given by the minimum energy criterion.

4.1 Inverse Compton emission

The CRe population seen in the radio band via synchrotron emission should also scatter photons of the cosmic microwave background (CMB), the local radiation field of elliptical galaxies, and the thermal X-ray emission of the ICM to different energy bands (Felten & Morrison 1966; Rees 1967). Combining measurements of inverse Compton (IC) and synchrotron emission eliminates the uncertainty in number density of the CRe population provided the inevitable extrapolation of the CRe power-law distribution for certain observed wavebands is justified. This enables the determination of the magnetic field strength B for an IC detection and a lower limit on B for a given non-detection of the IC emission.

The source function $q_{\rm IC}$ owing to IC scattering of CMB photons off an isotropic power law distribution of CRe (Eq. (2.1)) is (derived from Eq. (7.31) in Rybicki & Lightman 1979, in the case of Thomson scattering),

$$q_{\rm IC}(\boldsymbol{r}, E_\gamma) = \tilde{q}(\boldsymbol{r})\, f_{\rm IC}(\alpha_e) \left(\frac{m_{\rm e}\, c^2}{\rm GeV}\right)^{1-\alpha_{\rm e}} \left(\frac{E_\gamma}{kT_{\rm CMB}}\right)^{-(\alpha_\nu+1)}, \quad (4.1)$$

$$f_{\rm IC}(\alpha_e) = \frac{2^{\alpha_{\rm e}+3}\,(\alpha_{\rm e}^2+4\,\alpha_{\rm e}+11)}{(\alpha_{\rm e}+3)^2\,(\alpha_e+5)\,(\alpha_e+1)} \times \Gamma\left(\frac{\alpha_e+5}{2}\right)\zeta\left(\frac{\alpha_e+5}{2}\right), \quad (4.2)$$

$$\text{and } \tilde{q}(\boldsymbol{r}) = \frac{3\pi\,\sigma_{\rm T}\,\tilde{n}_{\rm CRe}(\boldsymbol{r})\;(kT_{\rm CMB})^2}{h^3\,c^2}, \quad (4.3)$$

where $\alpha_\nu = (\alpha_{\rm e}-1)/2$ denotes the spectral index, $\zeta(a)$ the Riemann ζ-function (Abramowitz & Stegun 1965), and $\tilde{n}_{\rm CRe}(\boldsymbol{r})$ is given by Eq. (2.2). After integrating over the considered energy interval and the IC emitting volume in the cluster, the particle flux $\mathcal{F}_\gamma(E_1, E_2)$ is obtained (c.f. Eq. (2.23)).

Enßlin & Biermann (1998) compiled non-detection limits of IC emission of different photon fields in various wavebands from the Coma cluster and obtained the tightest limits on B from the CMB photon field. The same CRe population emitting radio synchrotron radiation scatters CMB photons into the hard X-ray band. Non-detection of this IC emission by the OSSE experiment (Rephaeli et al. 1994) yields a lower limit on the central magnetic field strength of $B_{\rm Coma}(0) > 0.2\ \mu{\rm G}\ f_B^{-0.43}$, where f_B is the filling factor of the magnetic field in the volume occupied by CRe. Provided the CRe power-law distribution can be extrapolated to lower energies, the limit given by the EUV flux (Lieu et al. 1996) predicts a magnetic field strength stronger than $B_{\rm Coma}(0) > 1.2\ \mu{\rm G}\ f_B^{-0.43}$.

The reported high energy X-ray excess of the Coma cluster by the Beppo-Sax satellite (Fusco-Femiano et al. 1999) initiated other theoretical explanations about the origin of such an excess than IC up-scattering of CMB photons by relativistic electrons. One possibility implies the existence of a bremsstrahlung emitting suprathermal electron population between 10 and 100 keV which would also produce a unique Sunyaev-Zel'dovich signature (Enßlin et al. 1999; Enßlin & Kaiser 2000; Blasi et al. 2000; Blasi 2000; Liang et al. 2002; Colafrancesco et al. 2003). However, such a population is questioned on theoretical reasons (Petrosian 2001), and even the high X-ray excess of Coma itself is under debate (Rossetti & Molendi 2004; Fusco-Femiano et al. 2004). The data analysis of the RXTE observation of A 2256 yielded also evidence for a second spectral component (Rephaeli & Gruber 2003). On the basis of statistics alone, the detected emission is inconclusive as to whether it originates from a thermal multi-temperature fluid or an isothermal gas in combination with a non-thermal IC power-law emission. Future measurements with the IBIS instrument on-board the INTEGRAL satellite should provide even tighter upper limits respectively detections of the IC X-ray flux of a particular cluster and should therefore allow even tighter lower limits on the magnetic field strength.

4.2 γ-ray emission

This subsection outlines the method for estimating upper limits on the magnetic field strength using hadronic CRp interactions. The method is based on the idea of combining hadronically induced γ-ray and synchrotron emission to eliminate the uncertainty in number density of the CRp population. For this purpose, one necessarily needs to resolve the detailed broad spectral signature of γ-rays resulting from the π^0-decay (π^0-bump centred on $m_{\pi^0}c^2/2 \simeq 67.5$ MeV) as laid down in Eq. (2.20). This is to exclude other possible processes contributing to diffuse extended γ-ray emission like IC radiation or dark matter annihilation. Because of possible other additional contributions to the diffuse synchrotron emission from CRe populations, e.g. primarily accelerated electrons, we are only able to provide an upper limit on the magnetic field strength.

The proposed algorithm allows for different spatial resolutions of the γ-ray and synchrotron emission. The application, we have in mind, is the determination of intracluster magnetic fields. In this case, γ-ray observations of the π^0-decay induced γ-ray emission signature are only able to provide integrated γ-ray fluxes of the entire cluster due to their comparably large point spread function. γ-ray fluxes depend on the thermal electron density and temperature profiles which have to be derived from X-ray observations. However, if we assumed a comparable resolution in γ-ray and synchrotron emission the dependences on the thermal electron population could be eliminated (c.f. Sect. 2.2). The algorithm consists of the following two steps:

(i) Choosing a constant scaling parameter $X_{\rm CRp}$ for the CRp population and performing the volume integral of the energy integrated γ-ray source density λ_γ (2.20) yields the γ-ray flux according to Eq. (2.23). The CRp parameter $X_{\rm CRp}$ is obtained by comparing the observed to the theoretically expected γ-ray flux.

(ii) Inserting $X_{\rm CRp}$ into the synchrotron emissivity j_ν (2.7) enables us to solve for the magnetic field strength as function of angle on the sky when comparing to radio surface brightness observations.

Once a detailed angular distribution of π^0-decay induced γ-ray emission from a particular astrophysical object is available this algorithm may be implemented for the average of pixels contained within a certain solid angle. In this case the spatial distribution of CRp may even be deprojected.

Is there a chance to apply this method to galaxy cluster magnetic fields with future γ-ray instruments? Because of the necessity of resolving the broad spectral signature of γ-rays resulting from the π^0-decay centred on $\sim$ 67.5 MeV, the imaging atmospheric Čerenkov technique with a lower energy cutoff above 10 GeV is not applicable. Contrarily, the LAT instrument on-board GLAST scheduled to be launched in 2007 has an angular resolution better than 3.5° at 100 MeV while covering an energy range from 20 MeV up to 300 GeV with an energy resolution better than 10%. Assuming a photon spectral index of $\alpha_\gamma = 2$ for the γ-ray background, the point-source sensitivity at high galactic latitude in a one year

Table 1. Individual parameters describing the extended diffuse radio emission in the Coma and Perseus galaxy cluster according to Eq. (5.1). The maximal radius to which these profiles are applicable is denoted by $r_{\rm max}$. The radio data at 1.4 GHz are taken from Deiss et al. (1997) (Coma) and Pedlar et al. (1990) (Perseus) while the profile of the Coma cluster at 326 MHz is taken from Govoni et al. (2001) which is based on radio observations by Venturi et al. (1990).

Cluster	S_0 [Jy arcmin^{-2}]	$r_{\rm c}$ [h_{70}^{-1} kpc]	$r_{\rm max}$ [h_{70}^{-1} Mpc]	β
1.4 GHz observations:				
A1656 (Coma)	1.1×10^{-3}	450	1.0	0.78
A426 (Perseus)	2.3×10^{-1}	30	0.1	0.55
326 MHz observation:				
A1656 (Coma)	4.7×10^{-3}	850	0.7	1.07

all-sky survey is better than 6×10^{-9} cm^{-2} s^{-1} for energies integrated above 100 MeV. Specifically, assuming a CRp spectral index $\alpha_{\rm p} = 2.3$ and a flat $X_{\rm CRp}$ for simplicity, such a one year all-sky survey is able to constrain $X_{\rm CRp} < 0.01$ (Perseus) and $X_{\rm CRp} < 0.04$ (Coma). Taking additionally into account the γ-ray flux between 20 MeV and 100 MeV as well as a longer survey time will improve the sensitivities and yield even tighter limits on $X_{\rm CRp}$. Comparing to energetically favoured values $X_{\rm CRp_{min}}$ which are obtained by applying hadronic minimum energy arguments to a given radio synchrotron emission (c.f. Fig. 2 in Sect. 5) yields comparable values in the case of Perseus while the situation in Coma is less optimistic. However, a definitive answer to the applicability of this method can not be given on the basis of minimum energy arguments because such a minimum energy state is not necessarily realised in Nature.

5 APPLICATIONS

In this section we apply the classical and hadronic minimum energy criterion to the radio (mini-)halos of the Coma and Perseus galaxy clusters. For simplicity, the CRp and CRe spectral indices are assumed to be independent of position and therefore constant over the cluster volume. If a radial spectral steepening as reported by Giovannini et al. (1993) in the case of the Coma radio halo will be confirmed by future radio observations evincing a better signal-to-noise ratio, the CRp and CRe spectral index distributions would have to embody this additional degree of freedom. We discuss in Sect. 5.3 that a moderate steepening would not significantly modify the hadronic minimum energy condition while a strong steepening would challenge the hadronic scenario.

5.1 Classical minimum energy criterion

In a first step we have to deproject the radio surface brightness and electron density profiles: In analogy to X-ray observations we assume the azimuthally averaged radio profile to be described by a β-model,

$$S_\nu(r_\perp) = S_0 \left[1 + \left(\frac{r_\perp}{r_{\rm c}}\right)^2\right]^{-3\beta+1/2} . \quad (5.1)$$

Deprojecting this profile yields the radio emissivity (c.f. Appendix of Pfrommer & Enßlin 2004)

$$j_\nu(r) = \frac{S_0}{2\pi r_{\rm c}} \frac{6\beta-1}{(1+r^2/r_{\rm c}^2)^{3\beta}} \mathcal{B}\left(\frac{1}{2}, 3\beta\right) = j_{\nu,0}\left(1+r^2/r_{\rm c}^2\right)^{-3\beta} . \quad (5.2)$$

The individual parameters for the Coma radio halo and Perseus radio mini-halo are shown in Table 1. Both profiles describe the extended diffuse emission where all point sources have been subtracted. Particularly, the extremely bright flat-spectrum core owing to relativistic outflows of the radio galaxy NGC 1275 in the centre of the Perseus cluster has been excluded from the fit. The electron density profiles are inferred from X-ray observations by Briel et al. (1992) (Coma) and Churazov et al. (2003) (Perseus).

In the following, we assume that the energy distribution of the CRe population above a MeV is represented by a power-law in energy $E_{\rm e}$ with a lower cutoff. As a word of caution, such an assumption might be a strong simplification in the case of turbulent acceleration models yielding more complex energy distributions which are considerably flatter at lower energies (Brunetti et al. 2001; Petrosian 2001; Ohno et al. 2002) . We assume a CRe spectral index of $\alpha_{\rm e} = 3.3$ which translates into a synchrotron spectral index of $\alpha_\nu = 1.15$. This is consistent with radio data of Perseus and Coma; particularly when considering the spectral cutoff between 1 and 10 GHz owing to the Sunyaev-Zel'dovich flux decrement (Deiss et al. 1997; Enßlin 2002; Pfrommer & Enßlin 2004).

Applying the classical minimum energy criterion to the diffuse synchrotron emission of the Coma cluster yields a central magnetic field strength of $B_{\rm Coma}(r = 0) = 1.1^{+0.7}_{-0.4}$ μG. In the case of the Perseus radio mini-halo we obtain $B_{\rm Perseus}(r = 0) = 7.2^{+4.5}_{-2.8}$ μG. The indicated tolerance levels derive from the logarithmic definition of the theoretical accuracies of the minimum in Eq. (3.15). However, these values are highly dependent on the lower energy cutoff of the CRe population, E_1, and the CRp proportionality parameter $k_{\rm p}$. Following the philosophy of our paper we adopt a physically motivated lower Coulomb cutoff of the CRe distribution of $E_1 = 0.1$ GeV corresponding to a relativistic γ factor of $\gamma_{\rm e} \simeq 200$ (as suggested by Sarazin 1999). We also adopt a conservative choice of the proportionality constant between the CRe and CRp energy densities of $k_{\rm p} = 1$. An increase of $k_{\rm p}$ would directly increase the magnetic field strength by approximately the square root of this factor.

For a cluster-wide comparison of energy densities of magnetic fields, CRe, and CRp, it is convenient to introduce a scaling with the thermal energy density by means of

$$X_B(\boldsymbol{r}) \equiv \frac{x_B(\boldsymbol{r})}{x_{\rm th}(\boldsymbol{r})} = \frac{\varepsilon_B(\boldsymbol{r})}{\varepsilon_{\rm th}(\boldsymbol{r})}, \text{ and} \quad (5.3)$$

$$X_{\rm CRp,CRe}(\boldsymbol{r}) \equiv \frac{x_{\rm CRp,CRe}(\boldsymbol{r})}{x_{\rm th}(\boldsymbol{r})} = \frac{\varepsilon_{\rm CRp,CRe}(\boldsymbol{r})}{\varepsilon_{\rm th}(\boldsymbol{r})}. \quad (5.4)$$

Profiles of the CRe-to-thermal energy density $X_{\rm CRe_{min}}(r)$ and magnetic-to-thermal energy density $X_{B_{\rm min}}(r)$ are shown in Fig. 2 for the Coma and Perseus cluster and our different scenarios. The upper panels show the scaled energy densities in the acceleration model of CRe, obtained by the classical minimum energy criterion. While the optimal magnetic energy density is roughly a factor of two larger than the CRe energy density, they both can be in equipartition for the quasi-optimal case of their distribution of energy densities, as indicated by the dark shaded regions. In order to explain the observed synchrotron emission in the CRe acceleration scenario the CRe and magnetic energy densities are only required to be below one percent of the thermal energy density.

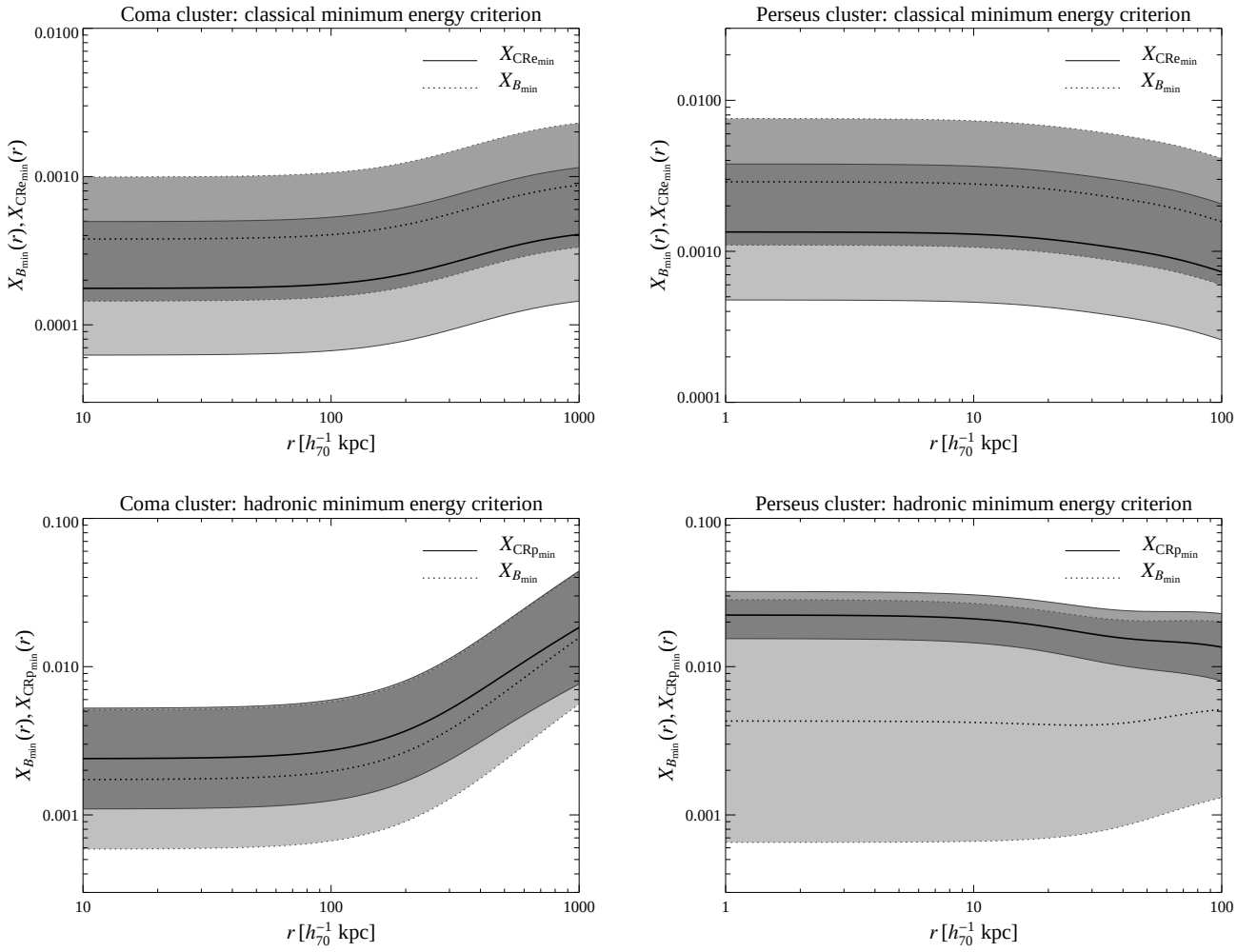

Figure 2. Profiles of the CRe-to-thermal energy density $X_{\mathrm{CRe_{min}}}(r)$ (solid) and magnetic-to-thermal energy density $X_{B_{\mathrm{min}}}(r)$ (dotted) as a function of deprojected radius are shown. The different energy densities are obtained by means of the classical minimum energy criterion (upper panels) and the hadronic minimum energy criterion (lower panels). In the latter scenario, profiles of the scaled CRp energy density are shown instead of CRe profiles. The left hand side shows profiles of the Coma cluster while the right hand side represents profiles of the Perseus cluster. The light shaded areas represent the logarithmic tolerance regions of $X_{B_{\mathrm{min}}}(r)$ and $X_{\mathrm{CRe_{min}}}(r)$, respectively, while the dark shaded regions indicate the overlap and thus the possible equipartition regions in the quasi-optimal case.

5.2 Hadronic minimum energy criterion

Assuming a CRp spectral index of $\alpha_{\mathrm{p}} = 2.3$ when applying the hadronic minimum energy criterion to the diffuse synchrotron emission of the Coma cluster yields a central magnetic field strength of $B_{\mathrm{Coma}}(r = 0) = 2.4^{+1.7}_{-1.0}$ μG. In the case of the Perseus cluster we obtain $B_{\mathrm{Perseus}}(r = 0) = 8.8^{+13.8}_{-5.4}$ μG. Both inferred profiles of the magnetic field are relatively flat: While the magnetic field strength in the outer part of the radio mini-halo in Perseus ($r \simeq 100\ h_{70}^{-1}$ kpc) declines to a value of 55% of its central value, the magnetic field in the outer region of the radio halo in Coma ($r \simeq 1\ h_{70}^{-1}$ Mpc) only decreases to 72% of its central value.

As discussed in Sect. 3.2.4, the hadronic scenario shows a increasing tolerance region for strong magnetic field strengths which are expected to be present in the case of cool core clusters, such as Perseus (Taylor & Perley 1993; Carilli & Taylor 2002; Vogt & Enßlin 2003). In this limit, synchrotron losses dominate over inverse Compton cooling. This almost cancels the dependence of the synchrotron emissivity on the magnetic energy density. The lower panels of Fig. 2 show the scaled energy densities $X_{B_{\mathrm{min}}}(r)$ and $X_{\mathrm{CRp_{min}}}(r)$ as inferred from the hadronic scenario. In both clusters the optimal CRp energy density is larger than the magnetic energy density within this model. However, both energy densities can be again in equipartition for the quasi-optimal case of their distribution, as indicated by the dark shaded regions.

Owing to the inverse dependence of $\sigma_{\ln x_B}$ and $\sigma_{\ln x_{\mathrm{CRp}}}$ on the magnetic energy density in the limit of strong magnetic fields (c.f. Eqs. (3.37) and (3.38)), a large tolerance region of $X_{B_{\mathrm{min}}}$ immediately implies a well defined localisation of $X_{\mathrm{CRp_{min}}}$. In the Perseus cluster this results in a confinement for the CRp energy density of 2% ± 1% of the thermal energy density. On the other hand, in the Coma cluster $X_{B_{\mathrm{min}}}(r)$ and $X_{\mathrm{CRp_{min}}}(r)$ are required to increase by less than one order of magnitude from the centre to the outer parts of the cluster in order to account for the observed radio halo. This increase might be partly due to azimuthally averaging the aspheric electron density distribution of the Coma cluster (Pfrommer & Enßlin 2004).

High values for the radio emissivity per target density and frequency C_{hadr} of order unity seem to reflect conditions in cool core clusters (formerly referred to as cooling flow cluster) whereas

smaller values seem to represent conditions in clusters without cool cores as shown in the following:

$$C_{\rm hadr} \equiv \frac{A_{E_{\rm p}}}{A_{E_{\rm syn}}} \frac{j_\nu}{A_{\varepsilon_{\rm eff}}} = C_{\rm cluster} \left(\frac{\nu}{1.4\,{\rm GHz}}\right)^{-1} \left(\frac{n_{\rm e}}{n_{\rm e,0}}\right)^{-1} \left(\frac{j_\nu}{j_{\nu,0}}\right), \qquad (5.5)$$

where $C_{\rm Coma} = 9.4 \times 10^{-4}$ and $C_{\rm Perseus} = 1.5 \times 10^{-1}$.

5.3 Possibility of a hadronic scenario in Perseus and Coma

5.3.1 Perseus radio mini-halo

The azimuthally averaged radio surface brightness profile of the Perseus mini-halo matches the expected emission by the hadronic scenario well on all radii (Pfrommer & Enßlin 2004) while requiring almost flat profiles for CRp and magnetic energy densities relative to the thermal energy density, $X_{\rm CRp}$ and X_B, respectively. Moreover, the small amount of required energy density in cosmic ray protons $\varepsilon_{\rm CRp}$ ($\sim 2\%$ relative to the thermal energy density) supports the hypothesis of a hadronic origin of the Perseus radio mini-halo not only because the hadronic minimum energy criterion predicts a close confinement of $\varepsilon_{\rm CRp}$ (see Sect. 5.2) but also because cosmological simulations carried out by Miniati et al. (2001) easily predict a CRp population at the clusters centre of this order of magnitude.

5.3.2 Coma radio halo

The energetically favoured radial profile for the magnetic field strength in the Coma cluster is almost flat as predicted by the hadronic minimum energy criterion (see Sect. 5.2). Provided these results would be realised in Nature, this apparently contradicts profiles of the magnetic field strength as inferred from numerical simulations which seem to follow the electron density $n_{\rm e}(r)$ according to $B(r) \propto n_{\rm e}(r)^{\alpha_B}$ with $\alpha_B \in [0.5, 0.9]$ (Dolag et al. 1999, 2001). It would also contradict theoretical considerations assuming the magnetic field to be frozen into the flow and isotropised, i.e. $\alpha_B = 2/3$ (Tribble 1993). Applying the flux freezing conditions to the electron density profile of Coma (Briel et al. 1992) yields an expected decline of the magnetic field strength from its central value to the magnitude at $1\,h_{70}^{-1}$ Mpc by a factor of ~ 6.7.

However, there are other numerical, physical, and observational arguments indicating large uncertainties in the origin, amplification mechanism, and specific profile of the magnetic field strength, thus leaving the hadronic scenario as a viable explanation of the Coma radio halo: In contrast to the cited numerical simulations, there are other cosmological simulations (Miniati 2001; Miniati et al. 2001) which are able to produce giant radio halos in the hadronic scenario and therefore reasonably flat profiles of the magnetic field strength. From the physical point of view, there could be stronger shear flows or a larger number of weaker shocks in the outer parts of clusters which are unresolved or not accounted for in current simulations. This would imply stronger additional amplification of the magnetic field strength in the outer parts of clusters yielding a flatter profile of the magnetic field strength. Observationally, there are still uncertainties in the radio surface profiles which are increased by azimuthally averaging the diffuse synchrotron emission in the presence of non-centrally symmetric emission components such as the so-called radio-bridge in Coma around NGC 4839.

In order to account for the radio halo of Coma in the hadronic scenario, the product of $X_{\rm CRp}$ and X_B needs to increase by nearly two orders of magnitude towards the outskirts of the halo (c.f. lower left panel of Fig. 2). Leaving aside the minimum energy criterion, this increase can be split arbitrarily among the magnetic and CRp energy density ratios. For instance a constant magnetic-to-thermal energy density ratio X_B, corresponding to $\alpha_B = 0.5$ in an isothermal cluster, is still consistent within the theoretically expected tolerance regions, i.e. within a quasi-optimal realisation. However, the CRp-to-thermal energy density ratio $X_{\rm CRp}$ would have to compensate for this by increasing nearly two orders of magnitude towards the outskirts of the halo.[4] This choice of the magnetic field morphology ($\alpha_B = 0.5$) has been adopted in Fig. 3 which represents a parameter study on the ability of hadronically originating CRe to generate the radio halo of Coma. Contour lines of $\max(X_{\rm CRp}) = (1, 0.3, 0.1, 0.03, 0.01)$ for the range $r \leqslant 1\,h_{70}^{-1}$ Mpc are shown in parameter space spanned by $\alpha_{\rm p}$ and B_0. The gradient of the maximum of $X_{\rm CRp}$ points downwards in Fig. 3 and thus leaves the upper region of parameter space where the hadronic scenario is energetically able to account for the observed radio halo. For the choice of $\alpha_{\rm p} = 2.3$ and $X_B = 0.01$ the maximum of the CRp-to-thermal energy density $X_{\rm CRp}$ is smaller than 3% for the entire range of the radio halo. Conservative choices for CRp spectral breaks have been adopted by means of Eq. (2.14): We assume a high-momentum break of $p_2 \sim 2 \times 10^7\,{\rm GeV}c^{-1}$ being derived from CRp diffusion (Berezinsky et al. 1997) while the lower momentum cut-off assumes the CRp to be accelerated from a thermal Maxwellian distribution, $p_1 \sim 3\sqrt{2 m_{\rm p} k T_{\rm Coma}} = 0.01\,{\rm GeV}c^{-1}$ (Miniati 2001). This choice of the lower cutoff represents the energetically tightest constraint because taking into account Coulomb losses would only weaken the energetic requirements. Moving away from the minimum energy solution, especially in the inner parts of the cluster,

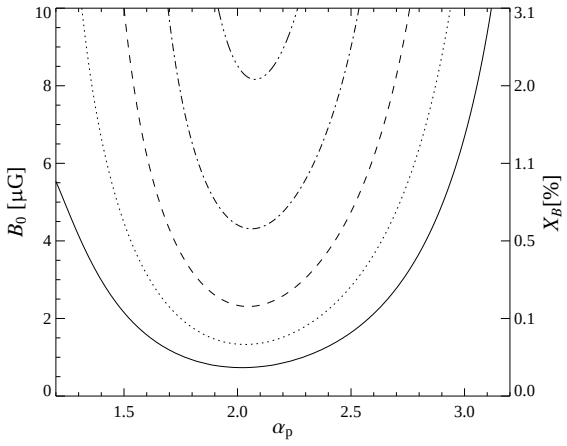

Figure 3. Parameter study on the ability of hadronically originating CRe to account for the radio halo of Coma. Assuming the profile of the magnetic field to scale with the square root of the electron density yields a flat magnetic-to-thermal energy density ratio X_B. Shown are contour lines from the bottom to the top of $\max(X_{\rm CRp}) = (1, 0.3, 0.1, 0.03, 0.01)$ for the range $r \leqslant 1\,h_{70}^{-1}$ Mpc in parameter space spanned by $\alpha_{\rm p}$ and B_0. Conservative choices for CRp spectral breaks have been assumed. The lower part represents the region in parameter space, where the hadronic scenario faces serious challenges for explaining the observed radio halo of Coma.

[4] Though, some part of this apparent increase is an artifact owing to azimuthally averaging the non-centrally symmetric synchrotron brightness distribution (for a more detailed discussion on this topic, see Pfrommer & Enßlin 2004).

the presented energetic considerations show that the hadronic scenario is a viable explanation of the Coma radio halo as long as the spatially constant CRp spectral index is between $1.4 \lesssim \alpha_{\rm p} \lesssim 2.8$.

Giovannini et al. (1993) found a strong radial spectral steepening from $\alpha_\nu = 0.8 - 1.8$ which would translate within the hadronic scenario into a CRp spectral index steepening of $\alpha_{\rm p} = 1.6 - 3.6$. If the strong steepening will be confirmed, the hadronic scenario will face serious challenges even when including conservative CRp spectral breaks. However, an absent or weaker steepening of the CRp spectral index e.g. from $\alpha_{\rm p} = 2.3$ in the cluster centre to $\alpha_{\rm p} = 2.8$ at the outskirts of the radio halo would only double the CRp energy density required to explain the radio halo in the hadronic scenario. The studies of Giovannini et al. (1993) are based on two synthesis aperture radio maps obtained with different radio telescopes. The technique of interferometric radio observations generally suffers from missing short-baseline information leading to an uncertainty of emission from larger structures: the so-called "missing zero spacing"-problem. This uncertainty of the surface brightness distribution at a single frequency is even increased for spatial distributions of the spectral index which represent a ratio of surface brightness distributions yielding to possible observational artefacts at the outskirts of the radio halo. Thus, future observations are required to decide whether the strong spectral steepening as a function of radius is an observational artifact or a real characteristic of the radio halo.

Figure 4 compares radio synchrotron profiles of the Coma radio halo by Govoni et al. (2001) which is based on observations by Venturi et al. (1990) using a synthesis aperture telescope with observations by Deiss et al. (1997) using a single-dish telescope. The statistical variance given by Govoni et al. (2001) represents the rms scatter within concentric annuli (shown in light grey) which is composed of measurement uncertainties and non-sphericity of the underlying radio profile. Rescaling with the square root of the number of independent beams within concentric annuli yields statistical uncertainties (black) however without taking into account systematics.[5] The top panel shows an comparison of the different profiles by Govoni et al. (2001) and Deiss et al. (1997) (rescaled from its original observational frequency $\nu = 1.4$ GHz to 326 MHz using the synchrotron spectral index $\alpha_\nu = 1.15$). There seems to be an indication of spectral steepening as reported by Giovannini et al. (1993). However, for simplicity we use a spatially constant CRp spectral index. Because of the more extended profile of the radio halo of the single-dish observation, we decided to adopt the profile obtained by Deiss et al. (1997) in our analysis shown in Fig. 2. Nevertheless, the lower panel of Fig. 4 shows a comparison of the energetically favoured magnetic-to-thermal energy density $X_{B_{\rm min}}(r)$ as a function of deprojected radius within the hadronic minimum energy criterion for both data sets. The tolerance regions of $X_{B_{\rm min}}$ are drawn light shaded while the overlap of $X_{B_{\rm min}}$ using the different synchrotron profiles is shown dark shaded. There is no significant difference within the allowed tolerance regions. Together with the previous considerations about spectral steepening, this indicates that a moderate radially dependent spectral index does not significantly modify the hadronic minimum energy condition while a strong steepening would challenge the hadronic scenario.

[5] Due to the interferometric nature of the measurement and due to the non-completely synthesised aperture, we expect the true error bars to be larger than the estimates given here suggest. However, a detailed discussion of this topic is beyond the scope of this work.

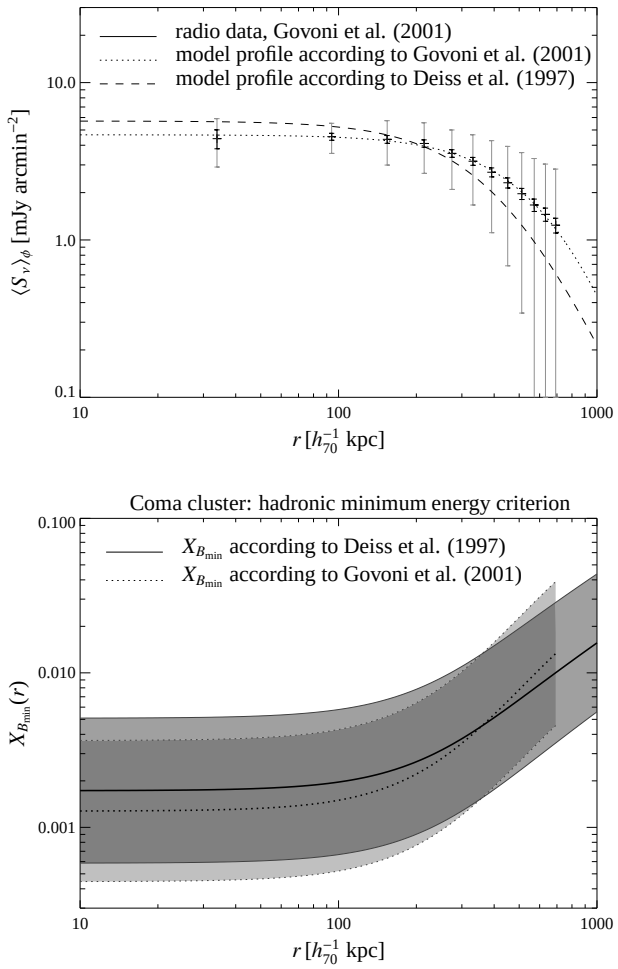

Figure 4. Top panel: Azimuthally averaged radio brightness profile of the radio halo in the Coma cluster as a function of impact parameter $r_\perp$. Shown are the radio data at 326 MHz (Govoni et al. 2001) in combination with the 1σ-error bars (black) and the surface brightness fluctuations within concentric annuli (grey) which are based on observations by Venturi et al. (1990). Also presented is the model profile according to Govoni et al. (2001) (dotted) and the model profile according to Deiss et al. (1997) (dashed) which is rescaled to 326 MHz using the synchrotron spectral index $\alpha_\nu = 1.15$ (c.f. Table 1). **Lower panel:** Profiles of the magnetic-to-thermal energy density $X_{B_{\rm min}}(r)$ in the Coma cluster as a function of deprojected radius are shown within the hadronic minimum energy criterion. A comparison of the used synchrotron profiles by Deiss et al. (1997) (solid, tolerance region medium grey shaded) and Govoni et al. (2001) (dotted, tolerance region light grey shaded) shows no significant difference within the allowed logarithmic tolerance regions (overlap is shown dark shaded).

6 MINIMUM ENERGY CRITERIA IN A NUTSHELL

This section provides self-consistent recipes for applying the classical and hadronic minimum energy criterion in typical observational situations. We present formulae for inferring magnetic field strengths solely as a function of observed flux per frequency, $\mathcal{F}_\nu$, luminosity distance to the galaxy cluster, D, extent of the cluster measured in core radius, $r_{\rm c}$, observed frequency, ν, and spectral index of the diffuse synchrotron emission, α_ν, where the emissivity scales as $j_\nu \propto \nu^{-\alpha_\nu}$.

The omnidirectional (i.e. integrated over 4π solid angle) lu-

minosity per frequency is given by the volume integral of the synchrotron emissivity, j_ν,

$$\mathcal{L}_\nu = 4\pi \int \mathrm{d}V\, j_\nu. \tag{6.1}$$

We choose a reference luminosity $\mathcal{L}_{\nu(1+z),0} = 4\pi D^2 (1+z)^{-1} \mathcal{F}_{\nu,0}$ which corresponds to a flux at $\nu = 1$ GHz of $\mathcal{F}_{\nu,0} = 1$ Jy for a source at a luminosity distance of $D = 100\ h_{70}^{-1}$ Mpc. This corresponds to a cluster like Coma which is characterised by a core radius of $r_{\mathrm{c},0} \sim 300\ h_{70}^{-1}$ kpc.

6.1 Classical minimum energy criterion in a nutshell

Applying the classical minimum energy criterion, we infer an optimal magnetic field strength by rewriting Eq. (3.11),

$$B_{\mathrm{min}}^{\mathrm{class}} = B_{\mathrm{min},0}^{\mathrm{class}}(\alpha_\nu)\ \mu\mathrm{G} \left[\frac{1+k_\mathrm{p}}{2} \frac{\mathcal{L}_\nu}{\mathcal{L}_{\nu,0}} \left(\frac{r_\mathrm{c}}{r_{\mathrm{c},0}} \right)^{-3} f_B^{-1} \times \left(\frac{\nu}{1\ \mathrm{GHz}} \right)^{\alpha_\nu} \left(\frac{E_1}{0.1\ \mathrm{GeV}} \right)^{1-2\alpha_\nu} \right]^{1/(\alpha_\nu+3)}. \tag{6.2}$$

Here $B_{\mathrm{min},0}^{\mathrm{class}}(\alpha_\nu)$ is given by Table 2, k_p denotes the ratio between CRp and CRe energy densities, E_1 denotes the lower cutoff of the CRe population, and f_B denotes the filling factor of the magnetic field in the volume occupied by CRe, which is thought to be of order unity. While deriving Eq. (6.2) we implicitly assumed that $E_2 \gg E_1$. We also applied a lower Coulomb cutoff to the CRe distribution of $E_1 = 0.1$ GeV (as suggested by Sarazin 1999), and adopt a conservative choice for the cosmic ray energy scaling of $k_\mathrm{p} = 1$.

In the case of the classical minimum energy criterion the tolerance region of the magnetic field strength is given by Eq. (3.16). The following substitutions might be useful when computing the tolerance levels of the magnetic field, $\sigma_{\ln B} = \sigma_{\ln x_B}/2$, which are equally spaced in logarithmic units of B. In linear representation of B, this definition explicitly implies the tolerance levels given by $\exp(\ln B \pm \sigma_{\ln B})$. The scaled synchrotron index is given by $\delta = (\alpha_\nu - 1)/2$, while the dimensionless magnetic energy density $x_{B_{\mathrm{min}}}^{\mathrm{class}}$ and the constant $C_{\mathrm{class}}(\alpha_\nu)$ are denoted by

$$x_{B_{\mathrm{min}}}^{\mathrm{class}} = \left(\frac{B_{\mathrm{min}}^{\mathrm{class}}}{B_\mathrm{c}} \right)^2 = \left(\frac{B_{\mathrm{min}}^{\mathrm{class}}}{31\ \mu\mathrm{G}} \right)^2 \left(\frac{\nu}{1\ \mathrm{GHz}} \right)^{-2}, \tag{6.3}$$

$$C_{\mathrm{class}}(\alpha_\nu) = f_{\mathrm{class}}(\alpha_\nu)\, f_B^{-1} \frac{\mathcal{L}_\nu}{\mathcal{L}_{\nu,0}} \left(\frac{r_\mathrm{c}}{r_{\mathrm{c},0}} \right)^{-3} \left(\frac{\nu}{1\ \mathrm{GHz}} \right)^{-3}, \tag{6.4}$$

where $f_{\mathrm{class}}(\alpha_\nu)$ is given by Table 2.

6.2 Hadronic minimum energy criterion in a nutshell

In the case of the hadronic scenario the energetically favoured magnetic field strength $B_{\mathrm{min},0}^{\mathrm{hadr}}$ is given by

$$B_{\mathrm{min},0}^{\mathrm{hadr}} = \sqrt{x_{B_{\mathrm{min}}}}\, B_\mathrm{c} = 31\ \mu\mathrm{G}\ \sqrt{x_{B_{\mathrm{min}}}} \left(\frac{\nu}{1\ \mathrm{GHz}} \right), \tag{6.5}$$

where $x_{B_{\mathrm{min}}}$ is given by Eqs. (3.28) through (3.31). $B_{\mathrm{min},0}^{\mathrm{hadr}}$ is specified in Table 2 for a few spectral indices α_ν where we assumed no cutoff of the CRp distribution. Provided the synchrotron index $\alpha_\nu \leqslant 1$, there must be an upper cutoff of the CRp distribution in order to ensure a non-divergent CRp energy density. This might be obtained by means of Eq. (2.14). Owing to the non-analytic structure of the hadronic minimum energy criterion (3.27) in $x_{B_{\mathrm{min}}}$, we were forced to carry out an asymptotic expansion for $x_{B_{\mathrm{min}}}$ which does not admit a comparable simple scaling of the magnetic field as in the classical case (6.2).

Table 2. Useful numerical values for particular choices of the synchrotron spectral index α_ν in the framework of the minimum energy criterion in a nutshell are given for both scenarios. Note, that a priori, we assume no cutoff in the CRp distribution. For spectral indices $\alpha_\nu \leqslant 1$ within the hadronic scenario, an upper cutoff needs to be introduced for deducing an equipartition magnetic field strength in order to meet the requirements of the regularity conditions.

α_ν	α_e	$B_{\mathrm{min},0}^{\mathrm{class}}$ [μG]	f_{class}	$B_{\mathrm{min},0}^{\mathrm{hadr}}$ [μG]	f_{hadr}
0.65	2.3	0.6	3.3×10^{-7}		
0.75	2.5	0.7	3.6×10^{-7}		
0.85	2.7	0.8	4.7×10^{-7}		
0.95	2.9	1.0	6.4×10^{-7}		
1.05	3.1	1.2	9.2×10^{-6}	4.0	2.1×10^{-2}
1.15	3.3	1.4	1.3×10^{-6}	4.2	1.9×10^{-2}
1.25	3.5	1.7	2.0×10^{-6}	5.3	3.4×10^{-2}
1.35	3.7	2.0	3.0×10^{-6}	7.3	8.2×10^{-2}
1.45	3.9	2.4	4.5×10^{-6}	13.0	3.9×10^{-1}

The theoretically expected tolerance levels of the magnetic field, $\sigma_{\ln B} = \sigma_{\ln x_B}/2$, are given by Eq. (3.32) while neglecting the radial dependence in the nutshell approach. The following substitutions might be useful when computing the magnetic field strength $B_{\mathrm{min},0}^{\mathrm{hadr}}$ and the corresponding tolerance region. The scaled synchrotron index is given by $\delta = (\alpha_\nu - 1)/2$, while the dimensionless energy density of the CMB, x_{CMB}, and the constant $C_{\mathrm{hadr}}(\alpha_\nu)$ are denoted by

$$x_{\mathrm{CMB}} = \frac{B_{\mathrm{CMB}}^2}{B_\mathrm{c}^2} = 1.08 \times 10^{-2} \left(\frac{\nu}{1\ \mathrm{GHz}} \right)^{-2} (1+z)^4, \tag{6.6}$$

$$C_{\mathrm{hadr}}(\alpha_\nu) = f_{\mathrm{hadr}}(\alpha_\nu)\, f_B^{-1} \frac{\mathcal{L}_\nu}{\mathcal{L}_{\nu,0}} \left(\frac{r_\mathrm{c}}{r_{\mathrm{c},0}} \right)^{-3} \left(\frac{n_\mathrm{e}}{n_{\mathrm{e},0}} \right)^{-1} \left(\frac{\nu}{1\ \mathrm{GHz}} \right)^{-3}, \tag{6.7}$$

where $f_{\mathrm{hadr}}(\alpha_\nu)$ is given by Table 2, and $n_{\mathrm{e},0} = 10^{-3}\ \mathrm{cm}^{-3}$.

7 CONCLUSIONS

We investigated the minimum energy criterion of radio synchrotron emission in order to estimate the energy density of magnetic fields with the main focus on the underlying physical scenario. The classical scenario might find application for cosmic ray electrons (CRe) originating either from primary shock acceleration or in-situ reacceleration processes while the hadronic model assumes a scenario of inelastic cosmic ray protons (CRp) interactions with the ambient gas of the intra-cluster medium (ICM) and thus leads to extended diffuse synchrotron and γ-ray emission.

Generally, the hadronic minimum energy estimates allow testing the hadronic model for extended radio synchrotron emission in clusters of galaxies. If it turns out that the required minimum non-thermal energy densities are too large compared to the thermal energy density, the hadronic scenario has to face serious challenges. For the classical minimum energy estimate, such a comparison can yield constraints on the accessible parameter space spanned by the lower energy cutoff of the CRe population or the unknown contribution of CRp to the non-thermal energy density.

For the first time we examine the localisation of the predicted minimum energy densities and provide a measure of the theoreti-

cally expected tolerance regions of these energetically favoured energy densities. The tolerance regions of the particular energy densities inferred from the classical minimum energy criterion are approximately constant for varying magnetic field strength ε_B. On the contrary, the hadronic minimum energy criterion predicts constant energy densities for varying magnetic field strength in the case of low ε_B compared to $\varepsilon_{\rm CMB}$, while the tolerance region of the CRp energy density decreases at the same rate as the tolerance region of ε_B increases for high ε_B.

Future observations should shed light on the hypothetical realisation of such an optimal distribution of energy densities in Nature: Combining upper limits on the inverse Compton (IC) scattering of cosmic microwave background photons off CRe electrons within the ICM provides lower limits on the magnetic field strength. Unambiguous detection of the π^0-decay induced γ-ray emission owing to hadronic CRp interactions in the ICM together with the observed radio synchrotron emission yields strong upper limits on the magnetic field strength. These are only upper limits because the inevitably accompanying hadronically generated CRe could have a non-hadronic counterpart CRe population which also contributes to the observed synchrotron emission. A combination of IC detection in hard X-rays, radio synchrotron emission, and hadronically induced γ-ray emission therefore simultaneously enables the determination of the CRp population as well as a bracketing of the total magnetic field strength and the CRe population. Applying the appropriate minium energy arguments would yield information about both the dynamical state as well as the fragmentation of the spatial distribution of the magnetic field.

Requiring the sum of cosmic ray and the magnetic field energy densities to be minimal for the observed synchrotron emission of the radio halo of the Coma cluster and the radio mini-halo of the Perseus cluster yields interesting results: Within the theoretically expected tolerance regions, equipartition is possible between the energy densities of CRp and magnetic fields, i.e. the minimum energy criterion always seems to choose equipartition to be a quasi-optimal case. Applying the hadronic minimum energy criterion to the diffuse synchrotron emission of the Coma cluster yields a central magnetic field strength of $B_{\rm Coma} = 2.4^{+1.7}_{-1.0}$ μG while in the case of the cool core cluster Perseus we obtain $B_{\rm Perseus} = 8.8^{+13.8}_{-5.4}$ μG. These values agree with magnetic field strengths inferred from Faraday rotation which range in the case of clusters without cool cores within [3 μG, 6 μG] while cool core clusters yield values of ~ 12 μG (Vogt & Enßlin 2003). Within the hadronic model for the radio mini-halo in the Perseus cluster, this results in a confinement for the CRp energy density of 2% ± 1% of the thermal energy density while the magnetic energy density reaches only 0.4% of the thermal energy density within large uncertainties. These energetic considerations show that the hadronic scenario is a very attractive explanation of cluster radio mini-halos.

In order to account for the radio halo of Coma in the hadronic scenario, the product of $\varepsilon_{\rm CRp}$ and ε_B needs to increase by nearly two orders of magnitude relative to the square of the thermal energy density $\varepsilon_{\rm th}$ towards the outskirts of the halo. Moving away from the minimum energy solution and adopting for instance a constant magnetic-to-thermal energy density, it is energetically possible to explain the observed synchrotron emission hadronically by only requiring the magnetic and CRp energy density to be a few per cent relative to the thermal energy density (and even less for the CRp in the cluster centre, provided $\alpha_{\rm p} \sim 2.3$ and the cluster is isothermal). Such a magnetic energy density corresponds to a central magnetic field strength of 6 μG. Assuming a lower magnetic field strength of 3 μG corresponding to a magnetic-to-thermal energy density of approximately 0.5% requires the CRp energy density to be lower than 10% for the entire range of the radio halo.

The considered hadronic scenario assumes a CRp spectral index which is independent of position and thus the radio emission does not show any spatial variations over the clusters volume. In principle, one could allow for radial spectral variations of the CRp and thereby for the radio emission by adopting a particular history of this population. For instance, one possible scenario would be given by continuous in-situ acceleration of CRp via resonant pitch angle scattering by turbulent Alfvén waves. We discuss that a moderate radial steepening would not significantly modify the hadronic minimum energy condition while a confirmation of the strong steepening reported by Giovannini et al. (1993) would seriously challenge the hadronic scenario.

As a caveat, it should be stressed that the inferred values for the particular energy densities only represent the energetically least expensive radio synchrotron emission model possible for a given physically motivated scenario. This minimum is not necessarily realised in Nature. Nevertheless, our minimum energy estimates are also interesting in a dynamical respect: Should the hadronic scenario of extended radio synchrotron emission be confirmed, the minimum energy estimates allow testing for the realisation of the minimum energy state for a given independent measurement of the magnetic field strength. Within the tolerance regions, our minimum energy estimates in Perseus and Coma agree well with magnetic field strengths inferred from Faraday rotation. Under the hypotheses of correctness of the hadronic scenario, such a possible realisation of the minimum energy state would seek an explanation of a first principle enforcing this extremal value to be realised in Nature.

ACKNOWLEDGEMENTS

The authors would like to thank Simon D. M. White, Matthias Bartelmann, Philip P. Kronberg, Björn Malte Schäfer, Corina Vogt and an anonymous referee for carefully reading the manuscript and their constructive remarks. This work was performed within the framework of the European Community Research and Training Network *The Physics of the Intergalactic Medium*.

REFERENCES

Abramowitz M., Stegun I. A., 1965, Handbook of mathematical functions. New York: Dover
Beck R., 2001, Space Science Reviews, 99, 243
Beck R., Brandenburg A., Moss D., Shukurov A., Sokoloff D., 1996, ARA&A, 34, 155
Berezinsky V. S., Blasi P., Ptuskin V. S., 1997, ApJ, 487, 529
Beuermann K., Kanbach G., Berkhuijsen E. M., 1985, A&A, 153, 17
Blasi P., 2000, ApJL, 532, L9
Blasi P., Colafrancesco S., 1999, Astroparticle Physics, 12, 169
Blasi P., Olinto A. V., Stebbins A., 2000, ApJL, 535, L71
Briel U. G., Henry J. P., Böhringer H., 1992, A&A, 259, L31
Brunetti G., 2002, in Bowyer S., Hwang C.-Y., eds, Matter and Energy in Clusters of Galaxies ASP Conference Series
Brunetti G., Blasi P., Cassano R., Gabici S., 2003, astro-ph/0312482
Brunetti G., Setti G., Comastri A., 1997, A&A, 325, 898
Brunetti G., Setti G., Feretti L., Giovannini G., 2001, MNRAS, 320, 365

Burbidge G. R., 1956, ApJ, 124, 416
Carilli C. L., Taylor G. B., 2002, ARA&A, 40, 319
Churazov E., Forman W., Jones C., Böhringer H., 2003, ApJ, 590, 225
Clarke T. E., Kronberg P. P., Böhringer H., 2001, ApJL, 547, L111
Colafrancesco S., Marchegiani P., Palladino E., 2003, A&A, 397, 27
Deiss B. M., Reich W., Lesch H., Wielebinski R., 1997, A&A, 321, 55
Dennison B., 1980, ApJL, 239, L93
Dermer C. D., 1986a, ApJ, 307, 47
Dermer C. D., 1986b, A&A, 157, 223
Dolag K., Bartelmann M., Lesch H., 1999, A&A, 348, 351
Dolag K., Enßlin T. A., 2000, A&A, 362, 151
Dolag K., Schindler S., Govoni F., Feretti L., 2001, A&A, 378, 777
Enßlin T. A., 2002, A&A, 396, L17
Enßlin T. A., Biermann P. L., 1998, A&A, 330, 90
Enßlin T. A., Biermann P. L., Kronberg P. P., Wu X.-P., 1997, ApJ, 477, 560
Enßlin T. A., Kaiser C. R., 2000, A&A, 360, 417
Enßlin T. A., Lieu R., Biermann P. L., 1999, A&A, 344, 409
Enßlin T. A., Röttgering H., 2002, A&A, 396, 83
Enßlin T. A., Vogt C., 2003, A&A, 401, 835
Felten J. E., Morrison P., 1966, ApJ, 146, 686
Fusco-Femiano R., dal Fiume D., Feretti L., Giovannini G., Grandi P., Matt G., Molendi S., Santangelo A., 1999, ApJL, 513, L21
Fusco-Femiano R., Orlandini M., Brunetti G., Feretti L., Giovannini G., Grandi P., Setti G., 2004, ApJL, in press
Giovannini G., Feretti L., Venturi T., Kim K. T., Kronberg P. P., 1993, ApJ, 406, 399
Giovannini G., Tordi M., Feretti L., 1999, New Astronomy, 4, 141
Gould R. J., 1972, Physica, 58, 379
Govoni F., Enßlin T. A., Feretti L., Giovannini G., 2001, A&A, 369, 441
Harris D. E., Kapahi V. K., Ekers R. D., 1980, A&AS, 39, 215
Iyudin A. F., Böhringer H., Dogiel V., Morfill G., 2004, A&A, 413, 817
Jaffe W. J., 1977, ApJ, 212, 1
Kuo P., Hwang C., Ip W., 2003, ApJ, 594, 732
Kuo P., Hwang C., Ip W., 2004, ApJ, in press
Liang H., Dogiel V. A., Birkinshaw M., 2002, MNRAS, 337, 567
Lieu R., Mittaz J. P. D., Bowyer S., Breen J. O., Lockman F. J., Murphy E. M., Hwang C. ., 1996, Science, 274, 1335
Miniati F., 2001, Computer Physics Communications, 141, 17
Miniati F., Jones T. W., Kang H., Ryu D., 2001, ApJ, 562, 233
Miniati F., Ryu D., Kang H., Jones T. W., 2001, ApJ, 559, 59
Ohno H., Takizawa M., Shibata S., 2002, ApJ, 577, 658
Pacholczyk A. G., 1970, Radio astrophysics. Nonthermal processes in galactic and extragalactic sources. Series of Books in Astronomy and Astrophysics, San Francisco: Freeman, 1970
Pedlar A., Ghataure H. S., Davies R. D., Harrison B. A., Perley R., Crane P. C., Unger S. W., 1990, MNRAS, 246, 477
Petrosian V. ., 2001, ApJ, 557, 560
Pfrommer C., Enßlin T. A., 2004, A&A, 413, 17
Pohl M., 1993, A&A, 270, 91
Rees M. J., 1967, MNRAS, 137, 429
Rephaeli Y., Gruber D., 2003, ApJ, 595, 137
Rephaeli Y., Ulmer M., Gruber D., 1994, ApJ, 429, 554
Rossetti M., Molendi S., 2004, A&A, 414, L41
Rybicki G. B., Lightman A. P., 1979, Radiative processes in astrophysics. New York, Wiley-Interscience, 1979.
Sarazin C. L., 1999, ApJ, 520, 529
Sarazin C. L., 2002, in ASSL Vol. 272: Merging Processes in Galaxy Clusters The Physics of Cluster Mergers. pp 1–38
Schlickeiser R., Sievers A., Thiemann H., 1987, A&A, 182, 21
Strong A. W., Moskalenko I. V., Reimer O., 2000, ApJ, 537, 763
Taylor G. B., Perley R. A., 1993, ApJ, 416, 554
Tribble P. C., 1993, MNRAS, 263, 31
Venturi T., Giovannini G., Feretti L., 1990, AJ, 99, 1381
Vestrand W. T., 1982, AJ, 87, 1266
Vogt C., Enßlin T. A., 2003, A&A, 412, 373
Völk H. J., Aharonian F. A., Breitschwerdt D., 1996, SSRv, 75, 279

This paper has been typeset from a TEX/ LATEX file prepared by the author.